Gravitational Waves and Dynamics of Coalescing Binary Systems

Thibault Damour

Institut des Hautes Etudes Scientifiques (Bures-sur-Yvette, France)

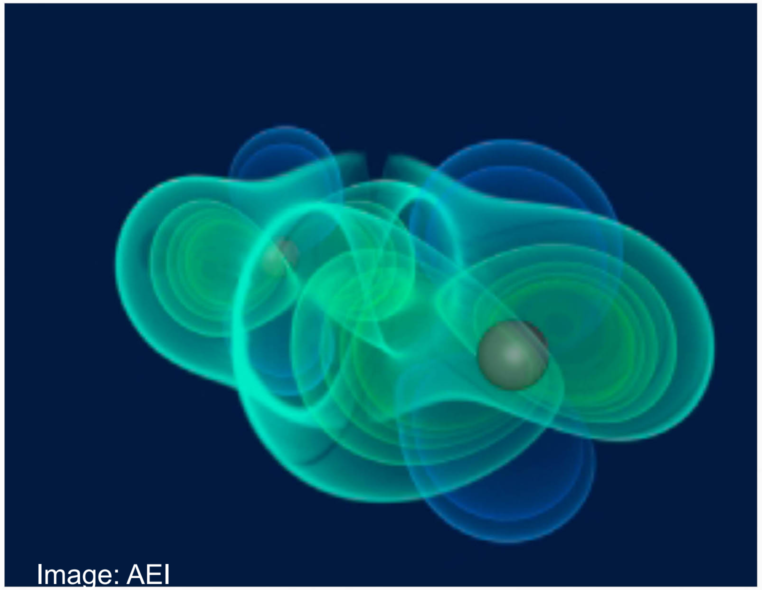

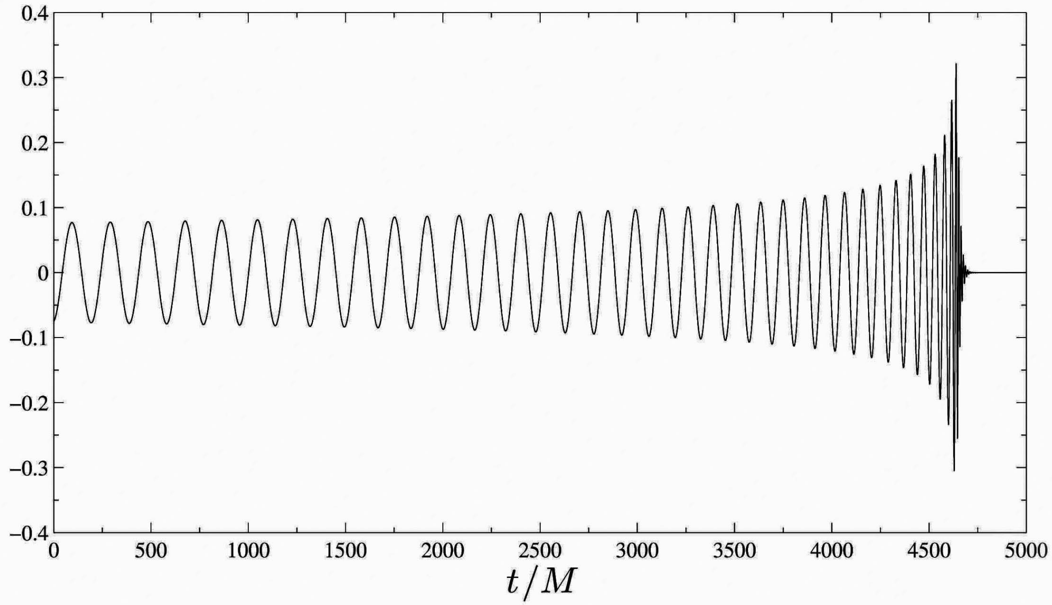

$$R_{\mu\nu} - \frac{1}{2} R g_{\mu\nu} = 8\pi G T_{\mu\nu}$$

Gravitational Waves in General Relativity (Einstein 1916,1918)

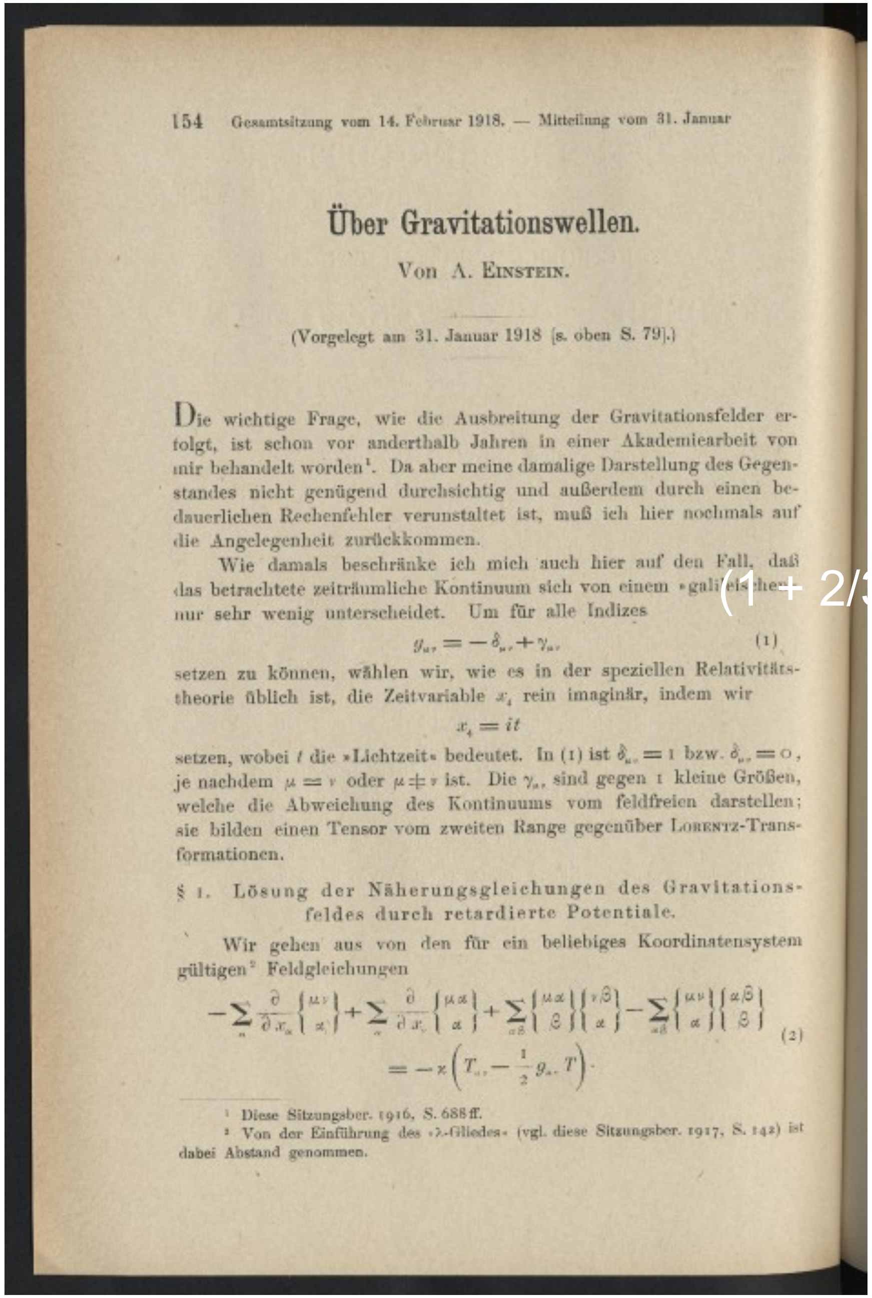

154 Gesamtsitzung vom 14. Februar 1918. — Mitteilung vom 31. Januar

Über Gravitationswellen.

Von A. Einstein.

(Vorgelegt am 31. Januar 1918 [s. oben S. 79].)

Die wichtige Frage, wie die Ausbreitung der Gravitationsfelder erfolgt, ist schon vor anderthalb Jahren in einer Akademiearbeit von mir behandelt worden[1]. Da aber meine damalige Darstellung des Gegenstandes nicht genügend durchsichtig und außerdem durch einen bedauerlichen Rechenfehler verunstaltet ist, muß ich hier nochmals auf die Angelegenheit zurückkommen.

Wie damals beschränke ich mich auch hier auf den Fall, daß das betrachtete zeiträumliche Kontinuum sich von einem »galileischen« nur sehr wenig unterscheidet. Um für alle Indizes

$$g_{\mu\nu} = -\delta_{\mu\nu} + \gamma_{\mu\nu} \qquad (1)$$

setzen zu können, wählen wir, wie es in der speziellen Relativitätstheorie üblich ist, die Zeitvariable x_4 rein imaginär, indem wir

$$x_4 = it$$

setzen, wobei t die »Lichtzeit« bedeutet. In (1) ist $\delta_{\mu\nu} = 1$ bzw. $\delta_{\mu\nu} = 0$, je nachdem $\mu = \nu$ oder $\mu \neq \nu$ ist. Die $\gamma_{\mu\nu}$ sind gegen 1 kleine Größen, welche die Abweichung des Kontinuums vom feldfreien darstellen; sie bilden einen Tensor vom zweiten Range gegenüber Lorentz-Transformationen.

§ 1. Lösung der Näherungsgleichungen des Gravitationsfeldes durch retardierte Potentiale.

Wir gehen aus von den für ein beliebiges Koordinatensystem gültigen[2] Feldgleichungen

$$-\sum_{\alpha} \frac{\partial}{\partial x_\alpha} \begin{Bmatrix} \mu\nu \\ \alpha \end{Bmatrix} + \sum_{\alpha} \frac{\partial}{\partial x_\nu} \begin{Bmatrix} \mu\alpha \\ \alpha \end{Bmatrix} + \sum_{\alpha\beta} \begin{Bmatrix} \mu\alpha \\ \beta \end{Bmatrix} \begin{Bmatrix} \nu\beta \\ \alpha \end{Bmatrix} - \sum_{\alpha\beta} \begin{Bmatrix} \mu\nu \\ \alpha \end{Bmatrix} \begin{Bmatrix} \alpha\beta \\ \beta \end{Bmatrix} = -\varkappa \left(T_{\mu\nu} - \frac{1}{2} g_{\mu\nu} T \right). \qquad (2)$$

[1] Diese Sitzungsber. 1916, S. 688 ff.

[2] Von der Einführung des »λ-Gliedes« (vgl. diese Sitzungsber. 1917, S. 142) ist dabei Abstand genommen.

$$g_{ij} = \delta_{ij} + h_{ij}$$

h_{ij}: transverse, traceless and propagates at v=c

Gravitational Waves: pioneering their detection

Joseph Weber (1919-2000)

General Relativity and Gravitational Waves
(Interscience Publishers, NY, 1961)

$$\frac{\delta L}{L} \approx h_{ij} n^i n^j$$

Gravitational Waves: two helicity states s=±2

Massless, two helicity states s=±2,
i.e. two Transverse-Traceless (TT) tensor polarizations propagating at v=c

$$h_{ij} = h_+(x_i x_j - y_i y_j) + h_\times(x_i y_j + y_i x_j)$$

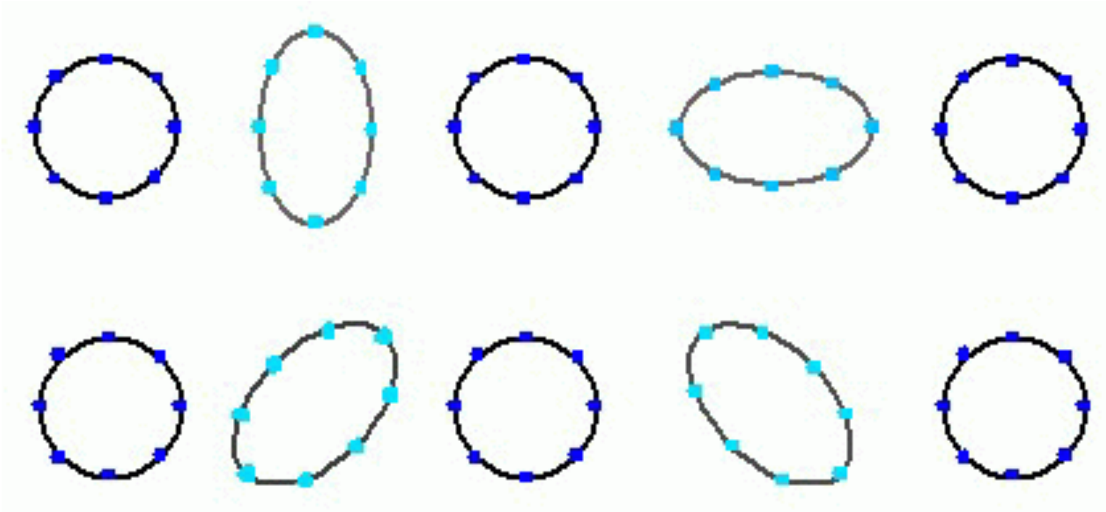

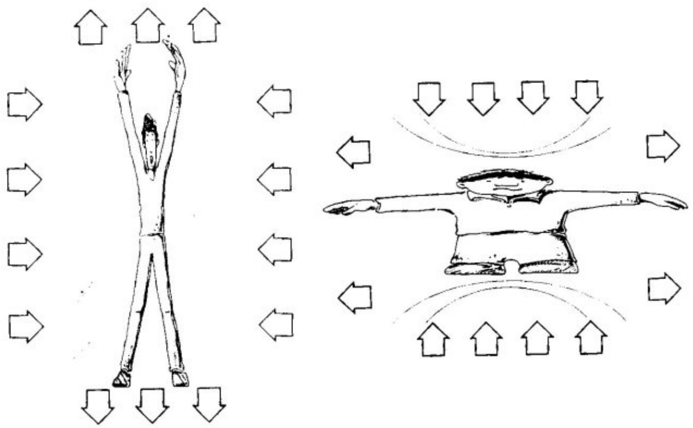

Binary Pulsar Tests I

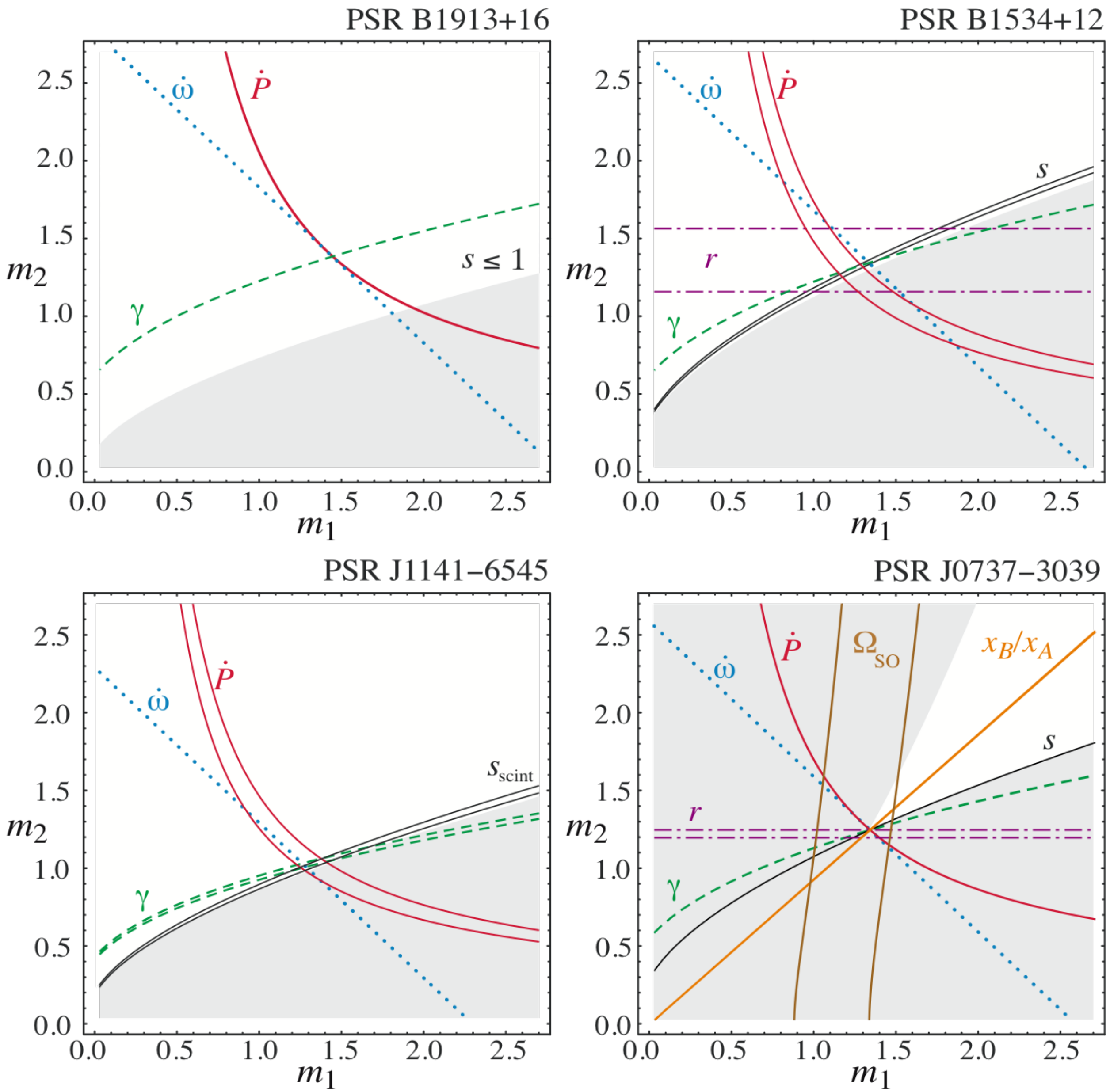

TD, Experimental Tests of Gravitational Theories, Rev. Part. Phys. 2013 update.

Binary Pulsar Tests II

Binary pulsar data have confirmed with 10^{-3} accuracy:

- The reality of gravitational radiation

- Several strong-field aspects of General Relativity

$$C_{NS} = \left(\frac{GM}{c^2 R_{NS}}\right) \approx 0.2$$ (Which is close to $C_{BH} = 0.5$)

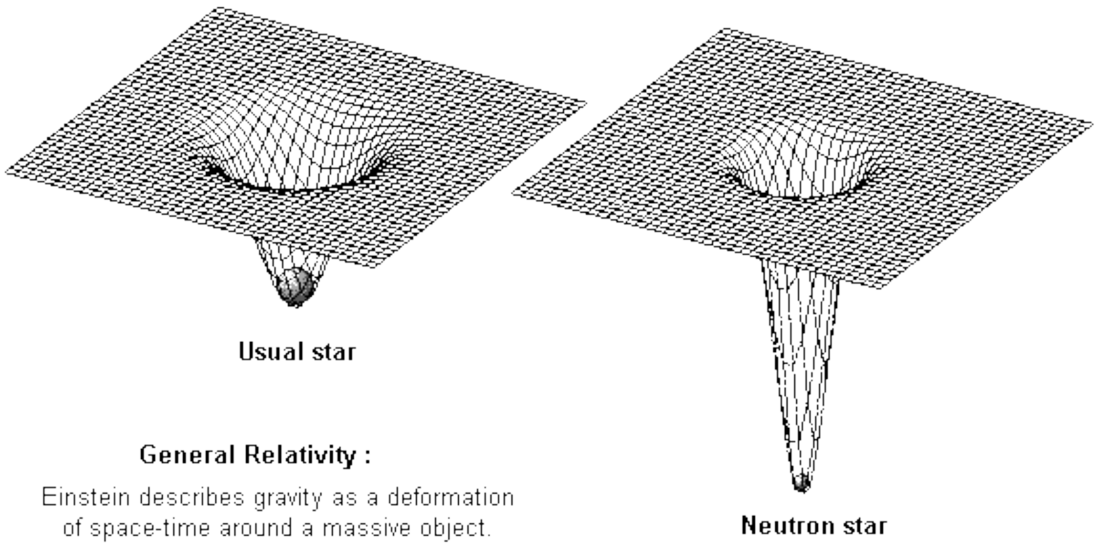

LASER INTERFEROMETER GW DETECTORS

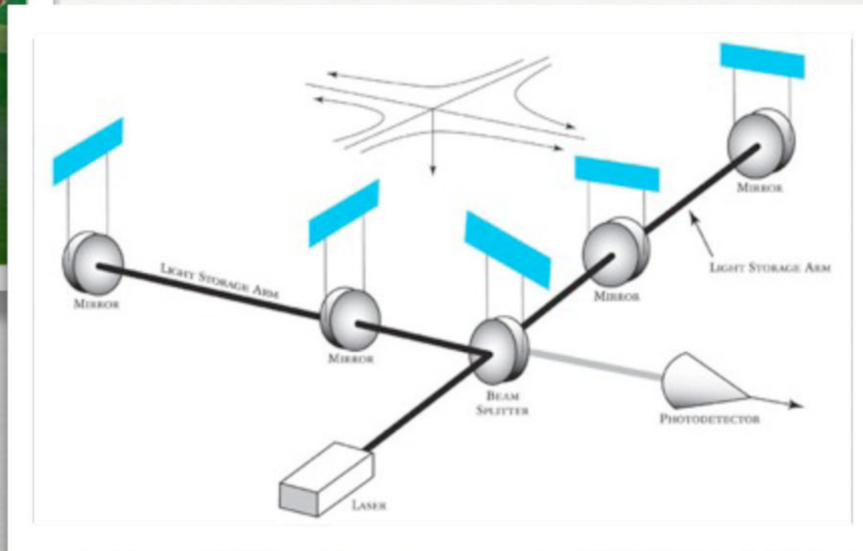

LIGO-VIRGO SENSITIVITY CURVES

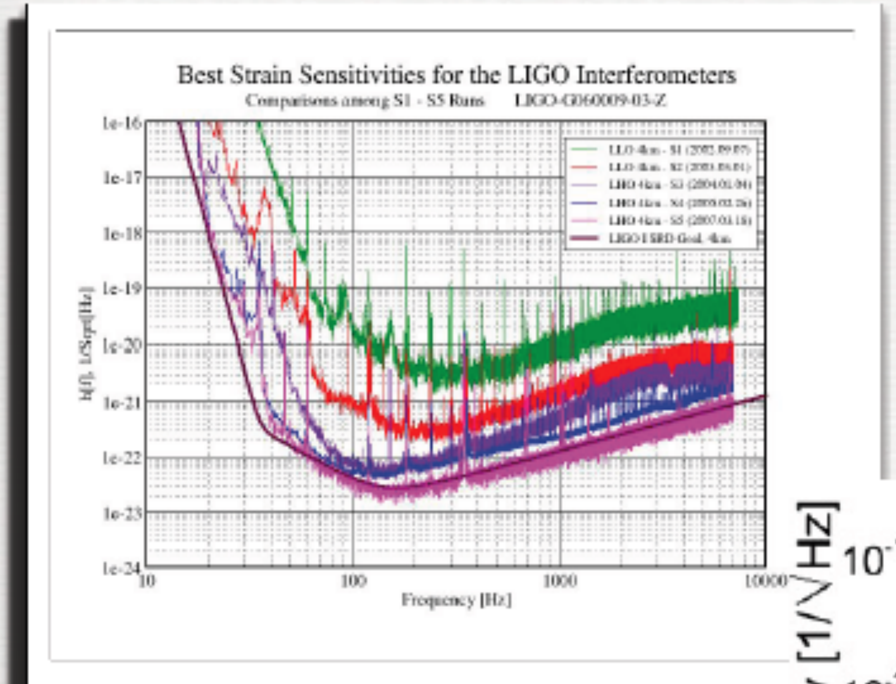

$$h = \frac{\delta L}{L} \approx 10^{-22}$$

$$\delta L \approx 10^{-17} \mathrm{cm}$$

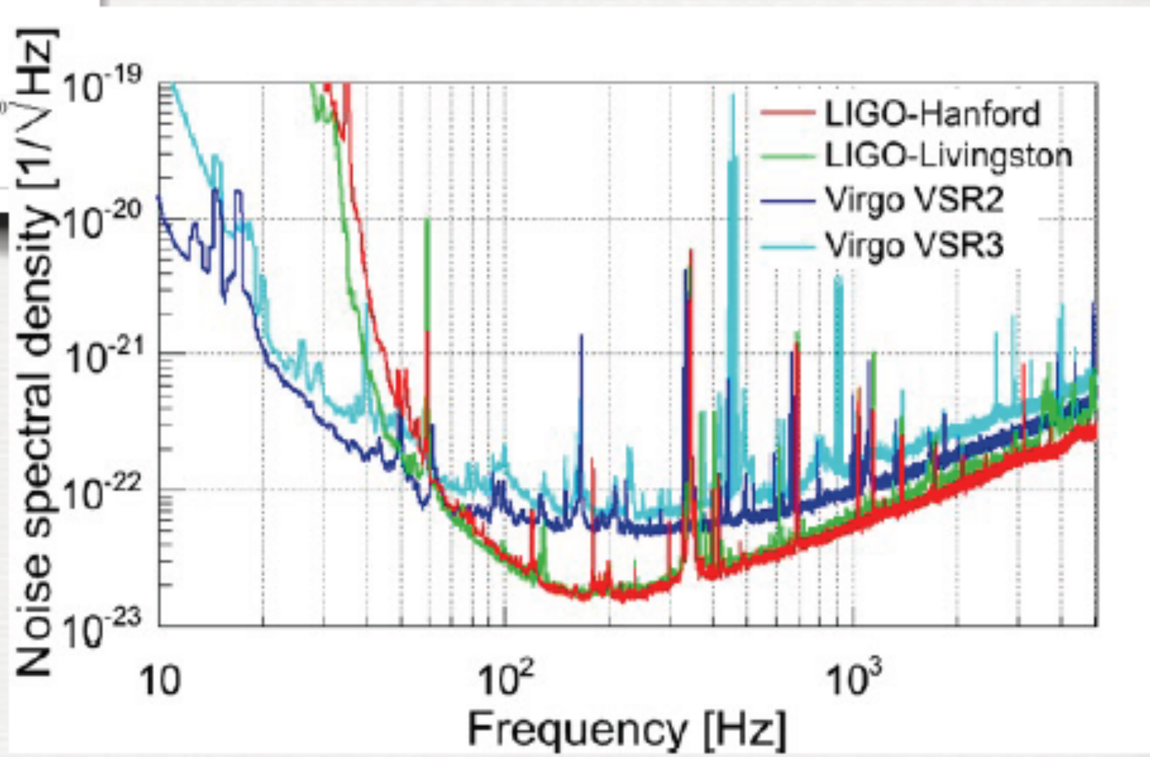

ADVANCED DETECTORS

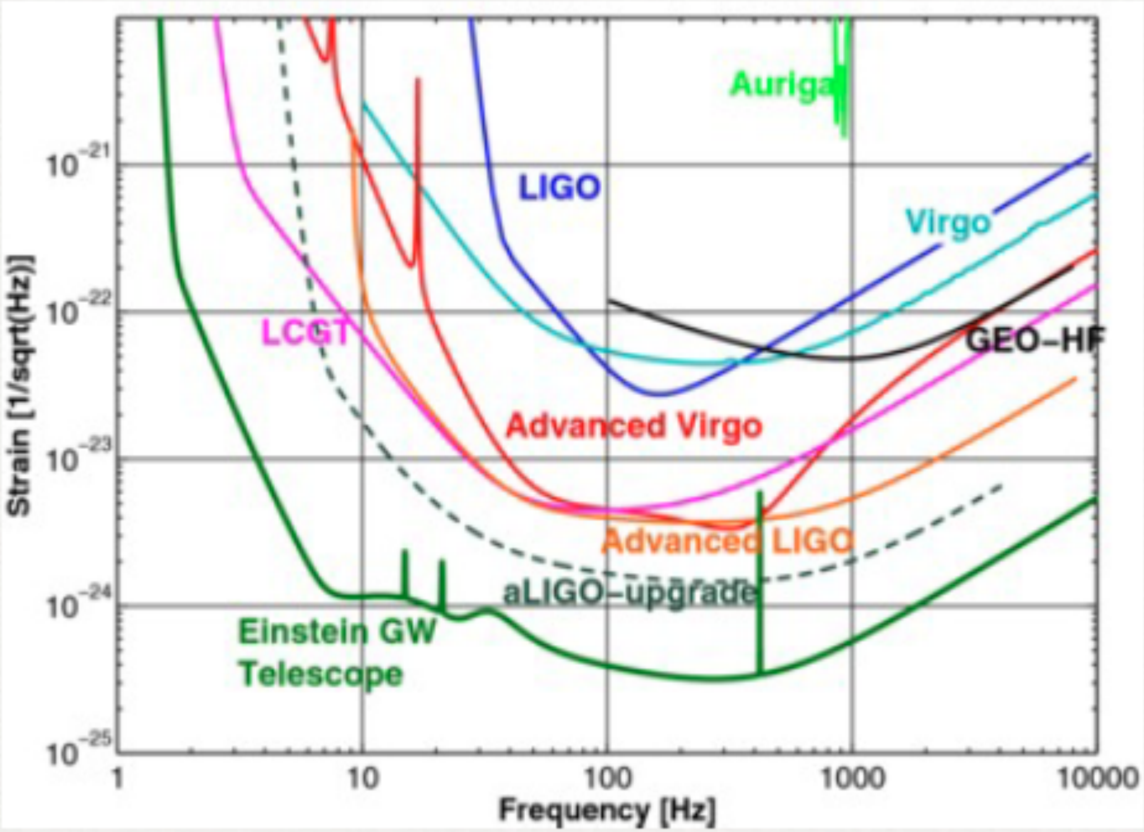

Gravitational wave sources : $h_{ij} \simeq \frac{2G}{c^4 r} \ddot{Q}^{TT}_{ij}(t - r/c)$

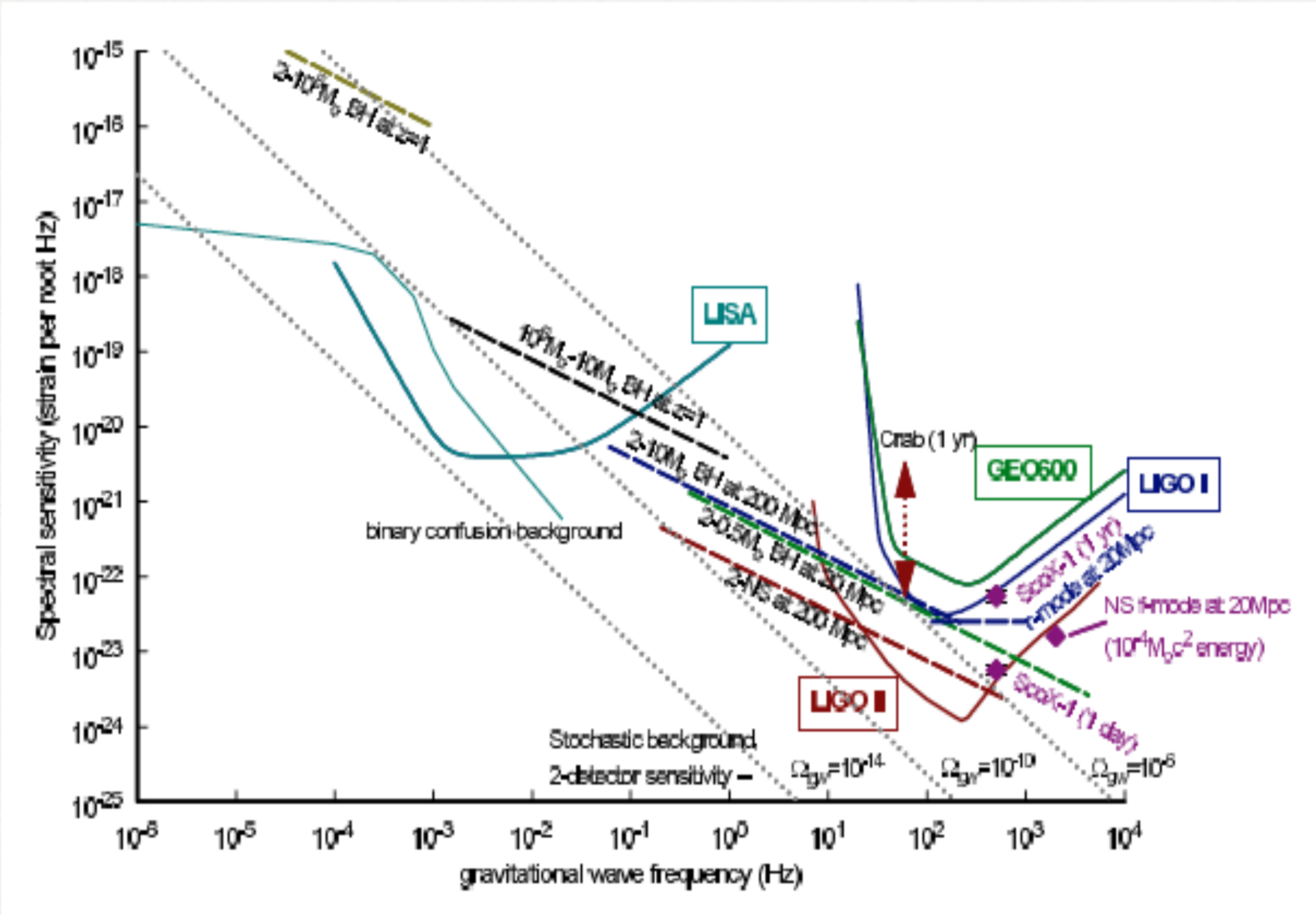

Sathyprakash&Schutz, Living Rev. Rel .12, 2009

Matched filtering technique

To extract GW signal from detector's output (lost in broad-band noise $S_n(f)$)

$$\boxed{\langle output \,|\, h_{template} \rangle = \int \frac{df}{S_n(f)} o(f) h^*_{template}(f)}$$

Template of expected GW signal

Detector's output

Need to know accurate representations of GW templates

The Problem of Motion in General Relativity

Solve

$$R_{\mu\nu} - \frac{1}{2} R \, g_{\mu\nu} = \frac{8\pi G}{c^4} T_{\mu\nu}$$

e.g. $$T^{\mu\nu} = (e+p)\, u^\mu u^\nu + p\, g^{\mu\nu}$$

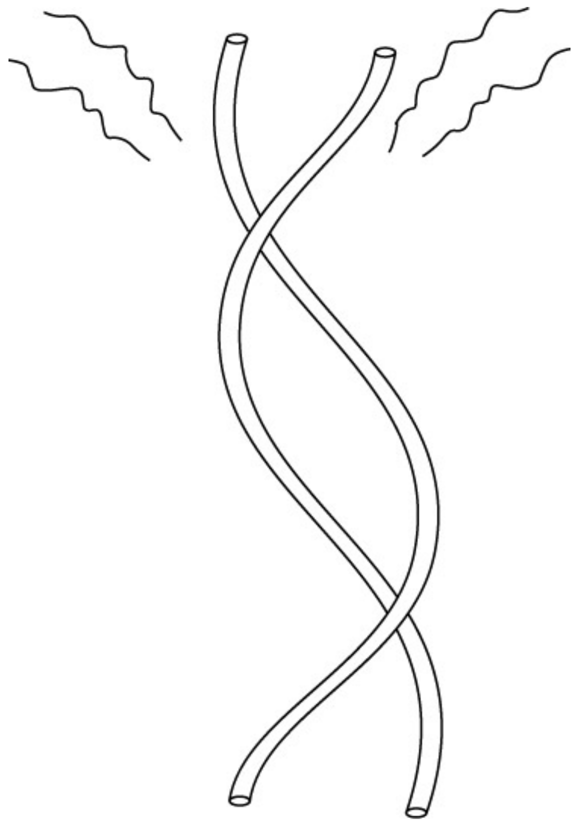

and extract physical results, e.g.

- Lunar laser ranging
- timing of binary pulsars
- gravitational waves emitted by binary black holes

The Problem of Motion in General Relativity (2)

Approximation Methods

- post-Minkowskian (Einstein 1916) $g_{\mu\nu}(x) = \eta_{\mu\nu} + h_{\mu\nu}(x)$, $h_{\mu\nu} \ll 1$
- post-Newtonian (Droste 1916) $h_{00} \sim h_{ij} \sim \frac{v^2}{c^2}$, $h_{0i} \sim \frac{v^3}{c^3}$, $\partial_0 h \sim \frac{v}{c} \partial_i h$
- Matching of asymptotic expansions body zone / near zone / wave zone
- Numerical Relativity

One-chart versus Multi-chart approaches

Coupling between Einstein field equations and equations of motion (Bianchi $\Rightarrow \nabla^\nu T_{\mu\nu} = 0$)

Strongly self-gravitating bodies : neutron stars or black holes : $h_{\mu\nu}(x) \sim 1$

Skeletonization : $T_{\mu\nu} \longrightarrow$ point-masses ? δ-functions in GR

Multipolar Expansion

Need to go to very high orders of approximation

Use a "cocktail": PM, PN, MPM, MAE, EFT, an. reg., dim. reg., …

Diagrammatic expansion of the interaction Lagrangian

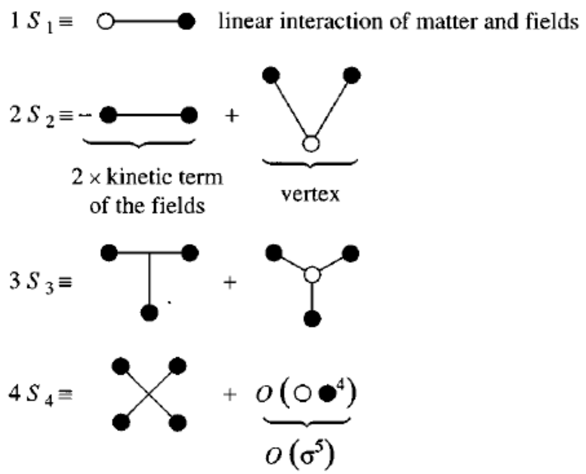

FIG. 4. Diagrammatic expression of the Φ^i-linear terms of the total action (3.6), for $i=1,2,3,4$.

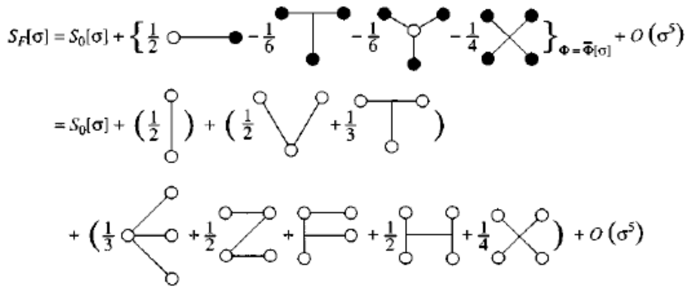

FIG. 6. Diagrammatic expansion of the Fokker action (3.13).

$$S_F[\sigma]=S_0[\sigma]+(\tfrac{1}{2}\,I)+(\tfrac{1}{2}\,V+\tfrac{1}{3}\,T)+(\tfrac{1}{3}\,\epsilon+\tfrac{1}{2}\,Z+F+\tfrac{1}{2}\,H$$
$$+\tfrac{1}{4}\,X)+O(\sigma^5). \qquad (3.14)$$

The most delicate term to compute would be the contribution due to the kinetic term of the fields in S_2, because one must expand up to order σ^3 the two fields Φ it involves. Fortunately, one can avoid estimating this term by using the Euler identity (3.12) to eliminate it from the Fokker action:

$$\begin{aligned}S_F[\sigma]&=[(S_0+S_1+S_2+\cdots)\\&\quad-\tfrac{1}{2}(S_1+2S_2+3S_3+\cdots)]_{\Phi=\bar{\Phi}[\sigma]}\\&=S_0+[\tfrac{1}{2}\,S_1-\tfrac{1}{2}\,S_3-S_4]_{\Phi=\bar{\Phi}[\sigma]}+O(\sigma^5).\end{aligned} \qquad (3.13)$$

The result of inserting Fig. 5 into Eq. (3.13) is displayed in Fig. 6. [The different diagrams have been drawn so that angles appear only at the vertices involving matter sources.] In the following, we will designate these diagrams by the letter they most naturally evoke, so that the final result for the Fokker action reads

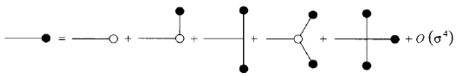

FIG. 5. Equation (3.2a) satisfied by the field $\bar{\Phi}[\sigma]$.

where R_{abcd} is the Riemann curvature of γ_{ab}. This choice cancels the term of order $\varphi\partial\varphi\partial\varphi$ in $S_{\text{spin }0}$, i.e., the "T"

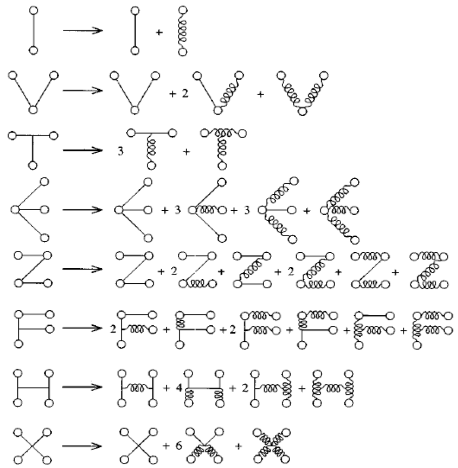

FIG. 7. Expression of the diagrams of Fig. 6 when the graviton and scalar propagators are represented respectively as curly and straight lines.

TD & G Esposito-Farèse, 1996

Templates for GWs from BBH coalescence

(Brady, Craighton, Thorne 1998)

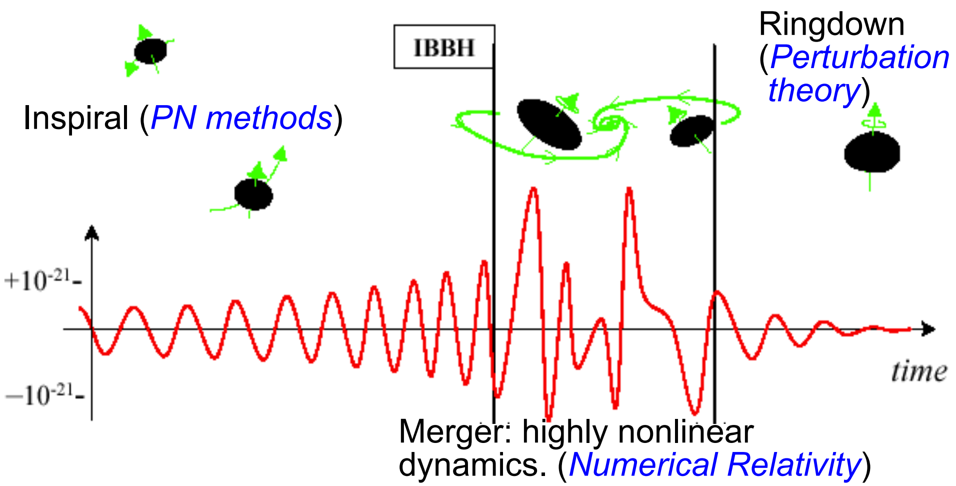

(Buonanno & Damour 2000)

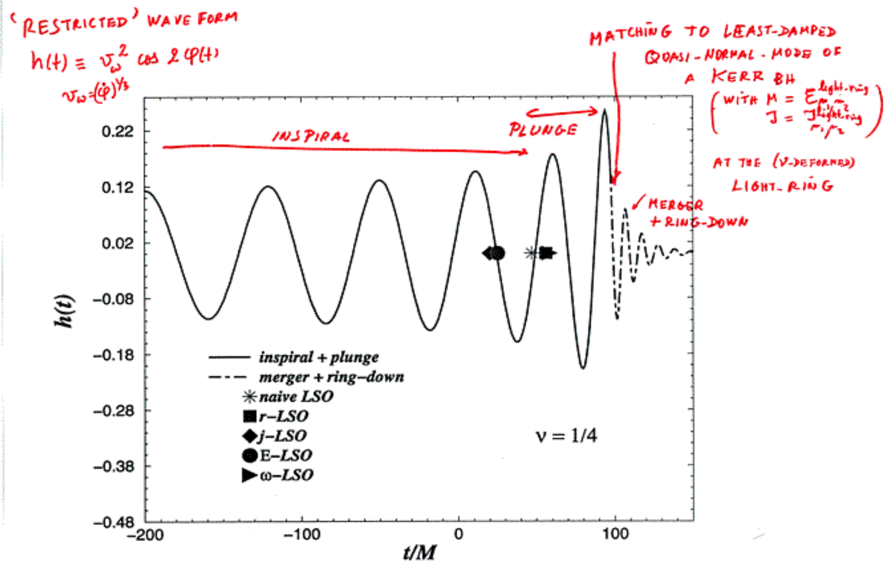

Numerical Relativity, the 2005 breakthrough:
Pretorius, Campanelli et al., Baker et al. …

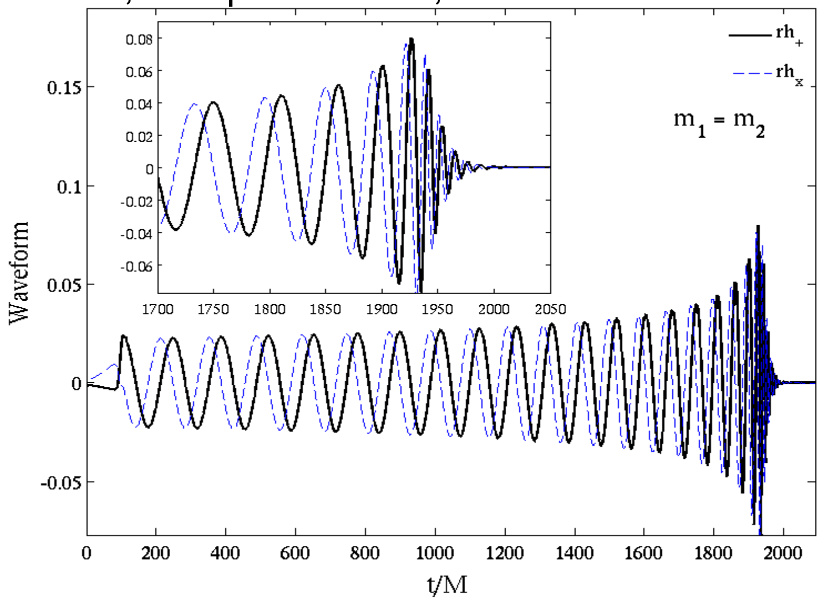

Binary black hole coalescence: Numerical Relativity

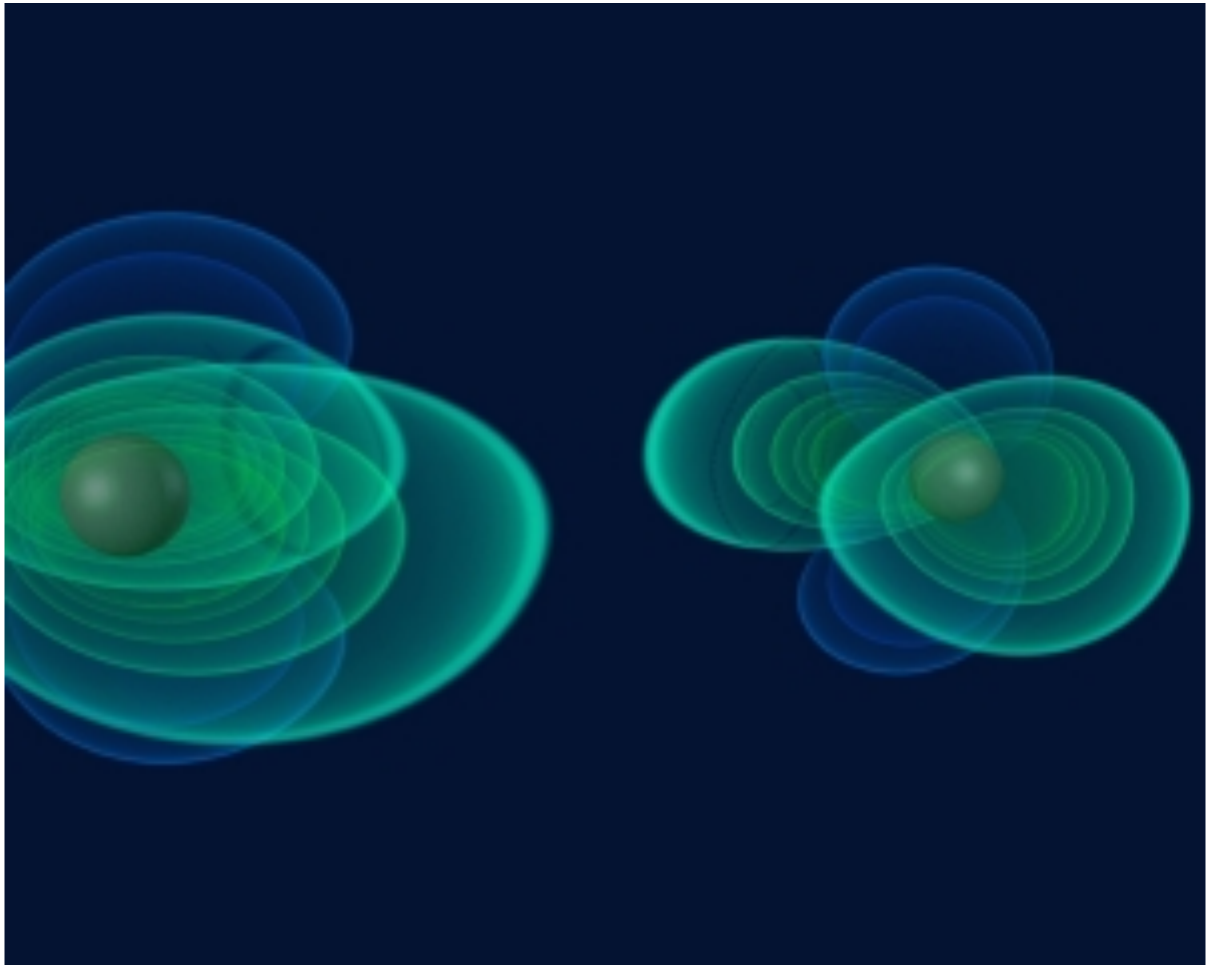

Image: AEI

NUMERICAL RELATIVITY WAVEFORM

Numerical Relativity: >= 2005 (Pretorius, Campanelli et al., Baker et al.)

Very accurate data: Caltech-Cornell spectral code (with some caveats): M. Scheel et al., 2008

Spectral code

Extrapolation (radius & resolution) Phase error: < 0.02 rad (inspiral) <0.1 ra (ringdown)

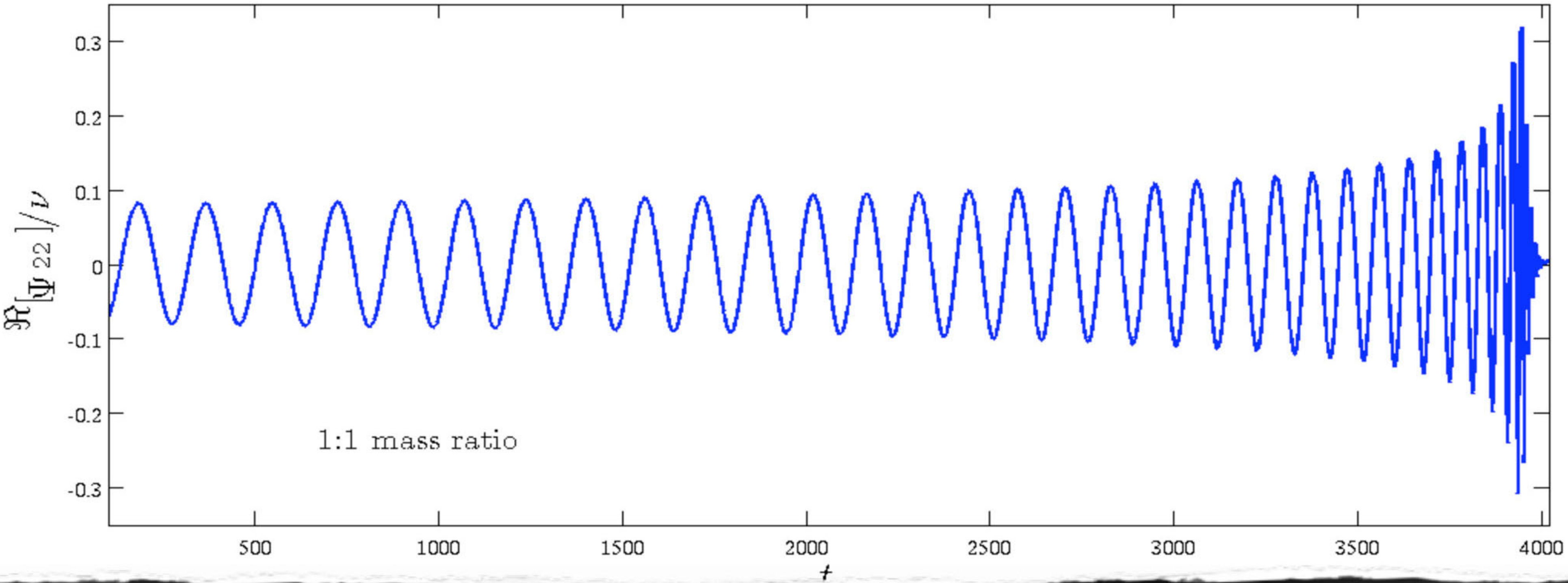

Importance of an analytical formalism

- **Theoretical:** physical understanding of the coalescence process, especially in complicated situations (arbitrary spins)

- **Practical:** need many thousands of accurate GW templates for detection & data analysis;
  need some "analytical" representation of waveform templates as $f(m_1,m_2,\mathbf{S}_1,\mathbf{S}_2)$

- Solution: **synergy between analytical & numerical relativity**

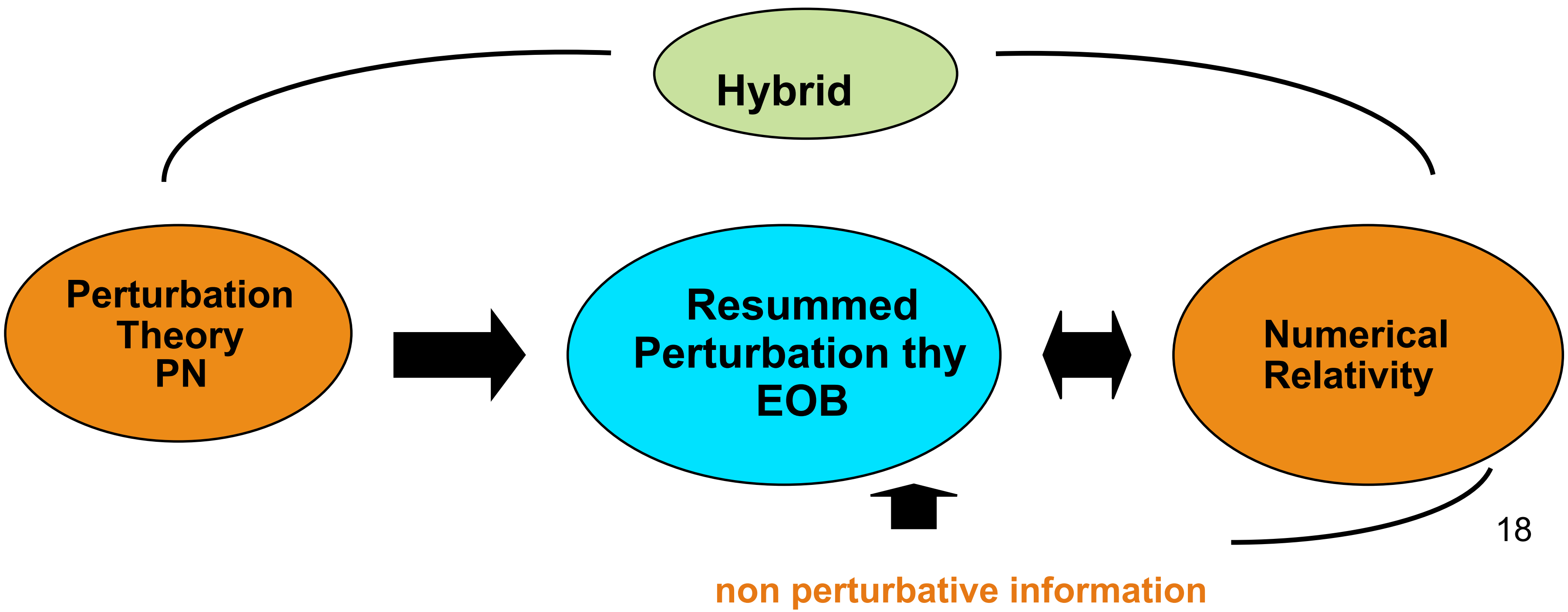

An improved analytical approach

EFFECTIVE ONE BODY (EOB)

approach to the two-body problem

Buonanno,Damour 99	(2 PN Hamiltonian)
Buonanno,Damour 00	(Rad.Reac. full waveform)
Damour, Jaranowski,Schäfer 00	(3 PN Hamiltonian)
Damour 01, Buonanno, Chen, Damour 05,…	(spin)
Damour, Nagar 07, Damour, Iyer, Nagar 08	(factorized waveform)
Buonanno, Cook, Pretorius 07, Buonanno, Pan …	(comparison to NR)
Damour, Nagar 10	(tidal effects)

Binary black hole coalescence: Analytical Relativity

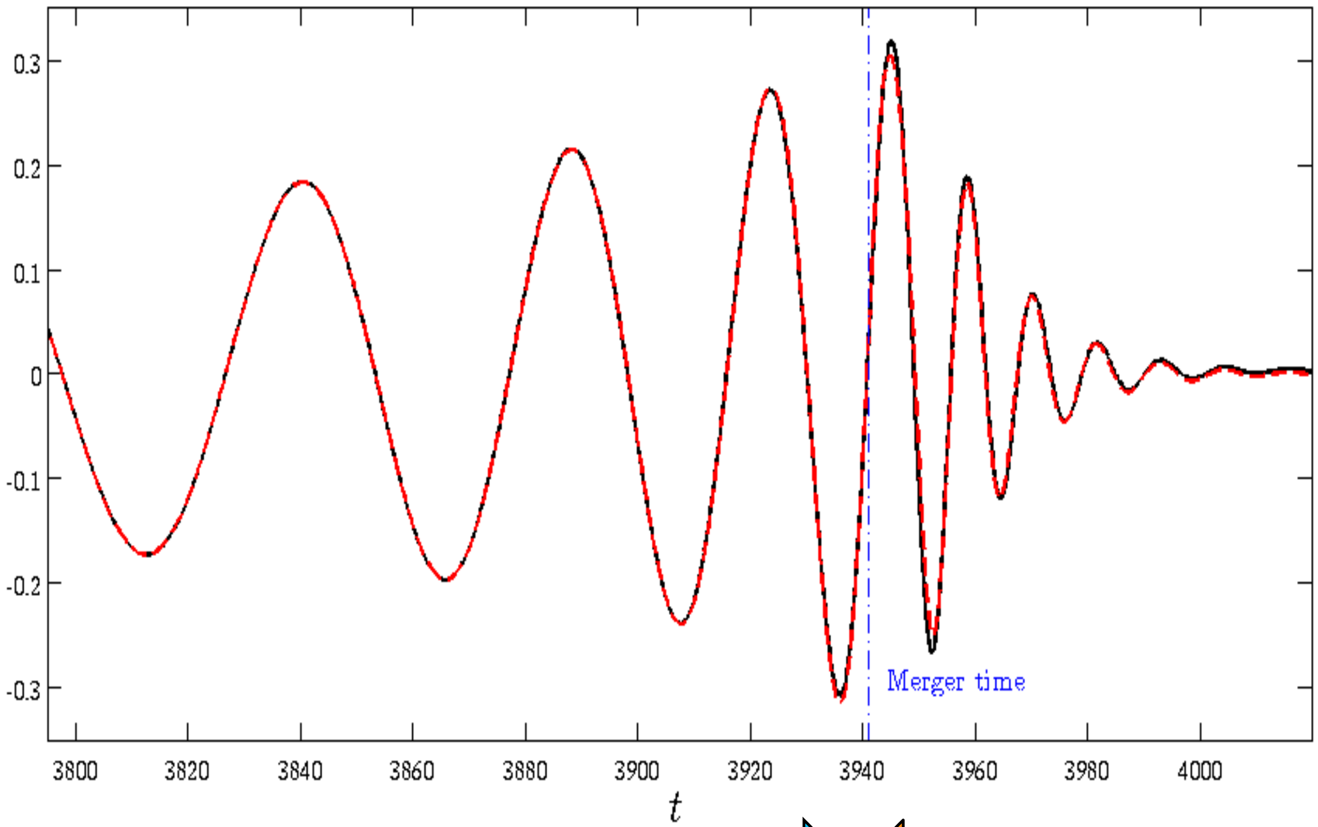

Inspiral + « plunge »

Ringdown

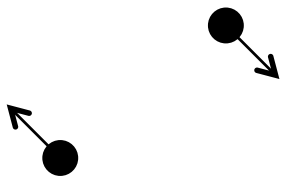

Two orbiting point-masses:
Resummed dynamics

Ringing BH

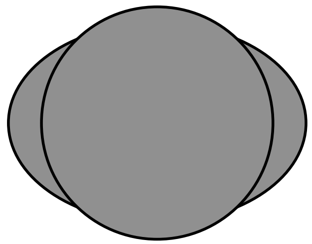

Motion of two point masses

$$S = \int d^D x \frac{R(g)}{16\pi G} - \sum_A \int m_A \sqrt{-g_{\mu\nu}(y_A) dy_A^\mu \, dy_A^\nu}$$

Dimensional continuation : $D = 4 + \varepsilon \ , \ \varepsilon \in \mathbb{C}$

Dynamics : up to 3 loops, i.e. 3 PN

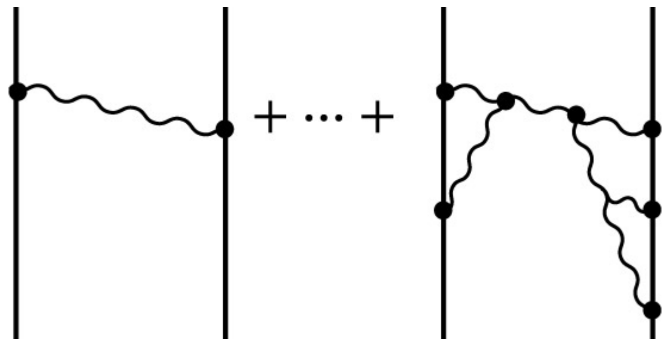

Jaranowski, Schäfer 98
Blanchet, Faye 01
Damour, Jaranowski Schäfer 01
Itoh, Futamase 03
Blanchet, Damour, Esposito-Farèse 04
Foffa, Sturani 11
4PN & 5PN log terms (Damour 10, Blanchet et al 11)
4PN (Jaranowski&Schaefer 13,
Foffa&Sturani 13, Bini&Damour 13)

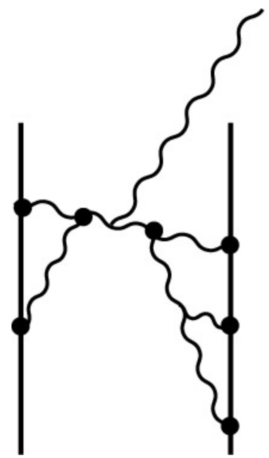

Radiation : up to 3 PN

Blanchet, Iyer, Joguet, 02,
Blanchet, Damour, Esposito-Farèse, Iyer 04
Blanchet, Faye, Iyer, Sinha 08

2-body Taylor-expanded 3PN Hamiltonian [JS98, DJS00,01]

$$H_{\rm N}(\mathbf{x}_a,\mathbf{p}_a) = \sum_a \frac{\mathbf{p}_a^2}{2\,m_a} - \frac{1}{2}\sum_a \sum_{b\neq a} \frac{G\,m_a\,m_b}{r_{ab}}\,.$$

$$H_{\rm 1PN}(\mathbf{x}_a,\mathbf{p}_a) = -\frac{1}{8}\frac{(\mathbf{p}_1^2)^2}{m_1^3} + \frac{1}{8}\frac{Gm_1m_2}{r_{12}}\left[-12\,\frac{\mathbf{p}_1^2}{m_1^2} + 14\,\frac{(\mathbf{p}_1\cdot\mathbf{p}_2)}{m_1m_2} + 2\,\frac{(\mathbf{n}_{12}\cdot\mathbf{p}_1)(\mathbf{n}_{12}\cdot\mathbf{p}_2)}{m_1m_2}\right] + \frac{1}{4}\frac{Gm_1m_2}{r_{12}}\frac{G(m_1+m_2)}{r_{12}} + (1\longleftrightarrow 2),$$

1PN

$$\begin{aligned}
H_{\rm 2PN}(\mathbf{x}_a,\mathbf{p}_a) = {}& \frac{1}{16}\frac{(\mathbf{p}_1^2)^3}{m_1^5} + \frac{1}{8}\frac{Gm_1m_2}{r_{12}}\left[5\,\frac{(\mathbf{p}_1^2)^2}{m_1^4} - \frac{11}{2}\frac{\mathbf{p}_1^2\,\mathbf{p}_2^2}{m_1^2m_2^2} - \frac{(\mathbf{p}_1\cdot\mathbf{p}_2)^2}{m_1^2m_2^2} + 5\,\frac{\mathbf{p}_1^2\,(\mathbf{n}_{12}\cdot\mathbf{p}_2)^2}{m_1^2m_2^2}\right.\\
&\left. -6\,\frac{(\mathbf{p}_1\cdot\mathbf{p}_2)\,(\mathbf{n}_{12}\cdot\mathbf{p}_1)(\mathbf{n}_{12}\cdot\mathbf{p}_2)}{m_1^2m_2^2} - \frac{3}{2}\frac{(\mathbf{n}_{12}\cdot\mathbf{p}_1)^2(\mathbf{n}_{12}\cdot\mathbf{p}_2)^2}{m_1^2m_2^2}\right]\\
&+\frac{1}{4}\frac{G^2m_1m_2}{r_{12}^2}\left[m_2\left(10\frac{\mathbf{p}_1^2}{m_1^2} + 19\frac{\mathbf{p}_2^2}{m_2^2}\right) - \frac{1}{2}(m_1+m_2)\frac{27\,(\mathbf{p}_1\cdot\mathbf{p}_2) + 6\,(\mathbf{n}_{12}\cdot\mathbf{p}_1)(\mathbf{n}_{12}\cdot\mathbf{p}_2)}{m_1m_2}\right]\\
&-\frac{1}{8}\frac{Gm_1m_2}{r_{12}}\frac{G^2(m_1^2+5m_1m_2+m_2^2)}{r_{12}^2} + (1\longleftrightarrow 2).
\end{aligned}$$

2PN

$$\begin{aligned}
H^{\rm reg}_{\rm 3PN}(\mathbf{x}_a,\mathbf{p}_a) = {}& -\frac{5}{128}\frac{(\mathbf{p}_1^2)^4}{m_1^7} + \frac{1}{32}\frac{Gm_1m_2}{r_{12}}\left[-14\,\frac{(\mathbf{p}_1^2)^3}{m_1^6} + 4\,\frac{\big((\mathbf{p}_1\cdot\mathbf{p}_2)^2 + 4\,\mathbf{p}_1^2\,\mathbf{p}_2^2\big)\mathbf{p}_1^2}{m_1^4m_2^2} + \frac{\big(\mathbf{p}_1^2\,\mathbf{p}_2^2 - 2\,(\mathbf{p}_1\cdot\mathbf{p}_2)^2\big)(\mathbf{p}_1\cdot\mathbf{p}_2)}{m_1^3m_2^3}\right.\\
&-10\,\frac{\big(\mathbf{p}_1^2\,(\mathbf{n}_{12}\cdot\mathbf{p}_2)^2 + \mathbf{p}_2^2\,(\mathbf{n}_{12}\cdot\mathbf{p}_1)^2\big)\mathbf{p}_1^2}{m_1^4m_2^2} + 24\,\frac{\mathbf{p}_1^2\,(\mathbf{p}_1\cdot\mathbf{p}_2)(\mathbf{n}_{12}\cdot\mathbf{p}_1)(\mathbf{n}_{12}\cdot\mathbf{p}_2)}{m_1^4m_2^2} + 2\,\frac{\mathbf{p}_1^2\,(\mathbf{p}_1\cdot\mathbf{p}_2)(\mathbf{n}_{12}\cdot\mathbf{p}_2)^2}{m_1^3m_2^3}\\
&+\frac{\big(7\,\mathbf{p}_1^2\,\mathbf{p}_2^2 - 10\,(\mathbf{p}_1\cdot\mathbf{p}_2)^2\big)(\mathbf{n}_{12}\cdot\mathbf{p}_1)(\mathbf{n}_{12}\cdot\mathbf{p}_2)}{m_1^3m_2^3} + 6\,\frac{\mathbf{p}_1^2\,(\mathbf{n}_{12}\cdot\mathbf{p}_1)^2(\mathbf{n}_{12}\cdot\mathbf{p}_2)^2}{m_1^4m_2^2}\\
&\left.+15\,\frac{(\mathbf{p}_1\cdot\mathbf{p}_2)(\mathbf{n}_{12}\cdot\mathbf{p}_1)^2(\mathbf{n}_{12}\cdot\mathbf{p}_2)^2}{m_1^3m_2^3} - 18\,\frac{\mathbf{p}_1^2\,(\mathbf{n}_{12}\cdot\mathbf{p}_1)(\mathbf{n}_{12}\cdot\mathbf{p}_2)^3}{m_1^3m_2^3} + 5\,\frac{(\mathbf{n}_{12}\cdot\mathbf{p}_1)^3(\mathbf{n}_{12}\cdot\mathbf{p}_2)^3}{m_1^3m_2^3}\right]\\
&+\frac{G^2m_1m_2}{r_{12}^2}\left[\frac{1}{16}(m_1-27m_2)\frac{(\mathbf{p}_1^2)^2}{m_1^4} - \frac{115}{16}m_1\frac{\mathbf{p}_1^2\,(\mathbf{p}_1\cdot\mathbf{p}_2)}{m_1^3m_2} + \frac{1}{48}m_2\frac{25\,(\mathbf{p}_1\cdot\mathbf{p}_2)^2 + 371\,\mathbf{p}_1^2\,\mathbf{p}_2^2}{m_1^2m_2^2}\right.\\
&+\frac{17}{16}\frac{\mathbf{p}_1^2(\mathbf{n}_{12}\cdot\mathbf{p}_1)^2}{m_1^3} - \frac{1}{8}m_1\frac{\big(15\,\mathbf{p}_1^2\,(\mathbf{n}_{12}\cdot\mathbf{p}_2) + 11\,(\mathbf{p}_1\cdot\mathbf{p}_2)\,(\mathbf{n}_{12}\cdot\mathbf{p}_1)\big)(\mathbf{n}_{12}\cdot\mathbf{p}_1)}{m_1^3m_2} + \frac{5}{12}\frac{(\mathbf{n}_{12}\cdot\mathbf{p}_1)^4}{m_1^3}\\
&-\frac{3}{2}m_1\frac{(\mathbf{n}_{12}\cdot\mathbf{p}_1)^3(\mathbf{n}_{12}\cdot\mathbf{p}_2)}{m_1^3m_2} + \frac{125}{12}m_2\frac{(\mathbf{p}_1\cdot\mathbf{p}_2)\,(\mathbf{n}_{12}\cdot\mathbf{p}_1)(\mathbf{n}_{12}\cdot\mathbf{p}_2)}{m_1^2m_2^2} + \frac{10}{3}m_2\frac{(\mathbf{n}_{12}\cdot\mathbf{p}_1)^2(\mathbf{n}_{12}\cdot\mathbf{p}_2)^2}{m_1^2m_2^2}\\
&\left.-\frac{1}{48}(220m_1+193m_2)\frac{\mathbf{p}_1^2(\mathbf{n}_{12}\cdot\mathbf{p}_2)^2}{m_1^2m_2^2}\right] + \frac{G^3m_1m_2}{r_{12}^3}\left[-\frac{1}{48}\left(466\,m_1^2 + \left(473-\frac{3}{4}\pi^2\right)m_1m_2 + 150\,m_2^2\right)\frac{\mathbf{p}_1^2}{m_1^2}\right.\\
&+\frac{1}{16}\left(77(m_1^2+m_2^2) + \left(143-\frac{1}{4}\pi^2\right)m_1m_2\right)\frac{(\mathbf{p}_1\cdot\mathbf{p}_2)}{m_1m_2} + \frac{1}{16}\left(61\,m_1^2 - \left(43+\frac{3}{4}\pi^2\right)m_1m_2\right)\frac{(\mathbf{n}_{12}\cdot\mathbf{p}_1)^2}{m_1^2}\\
&\left.+\frac{1}{16}\left(21(m_1^2+m_2^2) + \left(119+\frac{3}{4}\pi^2\right)m_1m_2\right)\frac{(\mathbf{n}_{12}\cdot\mathbf{p}_1)(\mathbf{n}_{12}\cdot\mathbf{p}_2)}{m_1m_2}\right]\\
&+\frac{1}{8}\frac{G^4m_1m_2^3}{r_{12}^4}\left[\left(\frac{227}{3}-\frac{21}{4}\pi^2\right)m_1 + m_2\right] + (1\longleftrightarrow 2). \qquad (12)
\end{aligned}$$

3PN

Taylor-expanded 3PN waveform

Blanchet,Iyer, Joguet 02, Blanchet, Damour, Esposito-Farese, Iyer 04, Kidder 07, Blanchet et al. 08

$$
\begin{aligned}
h^{22} = & -8\sqrt{\frac{\pi}{5}}\frac{G\nu m}{c^2R}e^{-2i\phi}x\Big\{1 - x\Big(\frac{107}{42} - \frac{55}{42}\nu\Big) + x^{3/2}\Big[2\pi + 6i\ln\Big(\frac{x}{x_0}\Big)\Big] - x^2\Big(\frac{2173}{1512} + \frac{1069}{216}\nu - \frac{2047}{1512}\nu^2\Big) \\
& - x^{5/2}\Big[\Big(\frac{107}{21} - \frac{34}{21}\nu\Big)\pi + 24i\nu + \Big(\frac{107i}{7} - \frac{34i}{7}\nu\Big)\ln\Big(\frac{x}{x_0}\Big)\Big] \\
& + x^3\Big[\frac{27\,027\,409}{646\,800} - \frac{856}{105}\gamma_E + \frac{2}{3}\pi^2 - \frac{1712}{105}\ln 2 - \frac{428}{105}\ln x \\
& - 18\Big[\ln\Big(\frac{x}{x_0}\Big)\Big]^2 - \Big(\frac{278\,185}{33\,264} - \frac{41}{96}\pi^2\Big)\nu - \frac{20\,261}{2772}\nu^2 + \frac{114\,635}{99\,792}\nu^3 + \frac{428i}{105}\pi + 12i\pi\ln\Big(\frac{x}{x_0}\Big)\Big] + O(\epsilon^{7/2})\Big\},
\end{aligned}
$$

$$x = (M\Omega)^{2/3} \sim v^2/c^2$$

$$
\boxed{
\begin{aligned}
M &= m_1 + m_2 \\
\nu &= m_1 m_2/(m_1 + m_2)^2
\end{aligned}
}
$$

Structure of EOB formalism

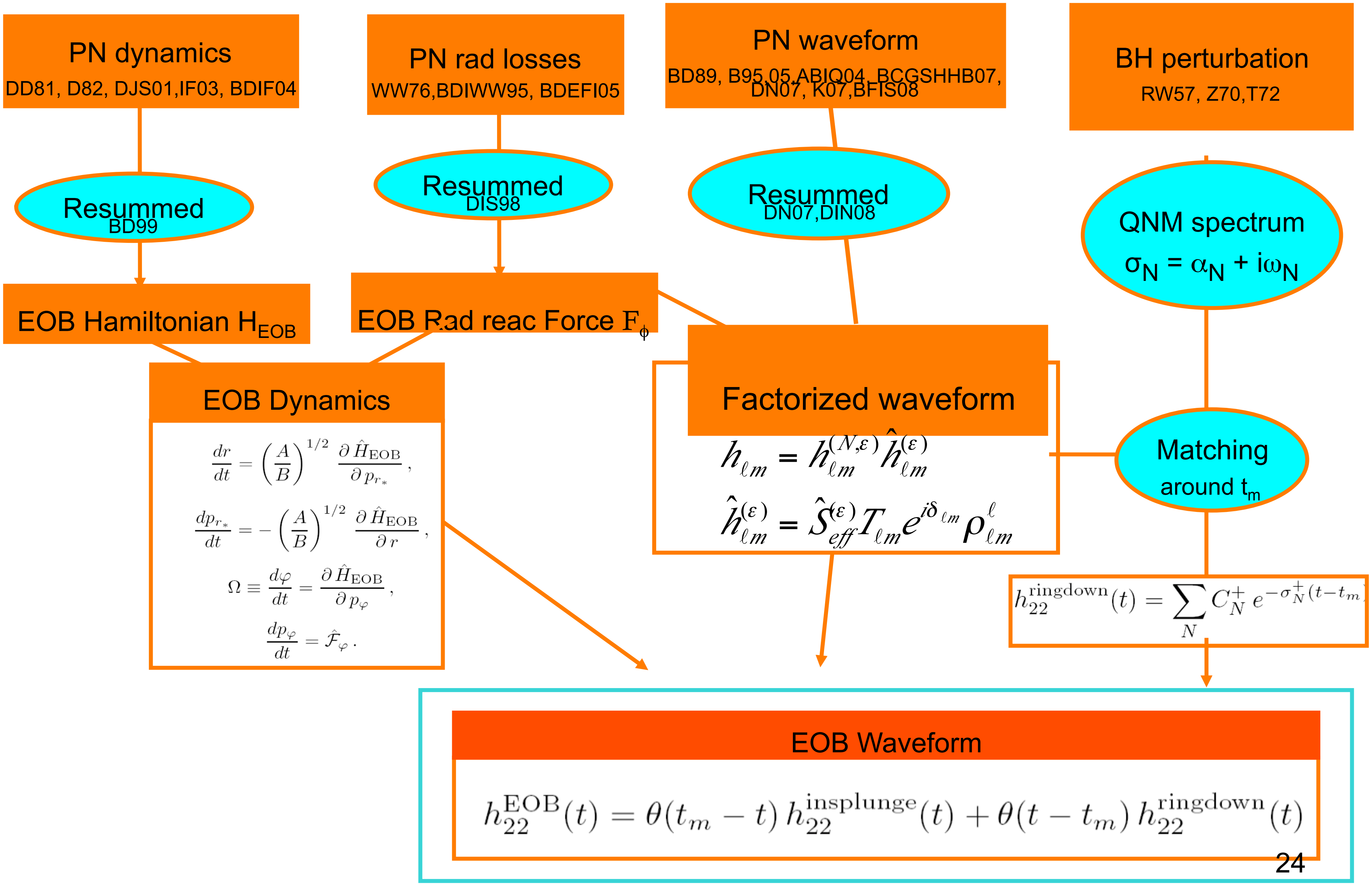

Real dynamics versus Effective dynamics

Real dynamics

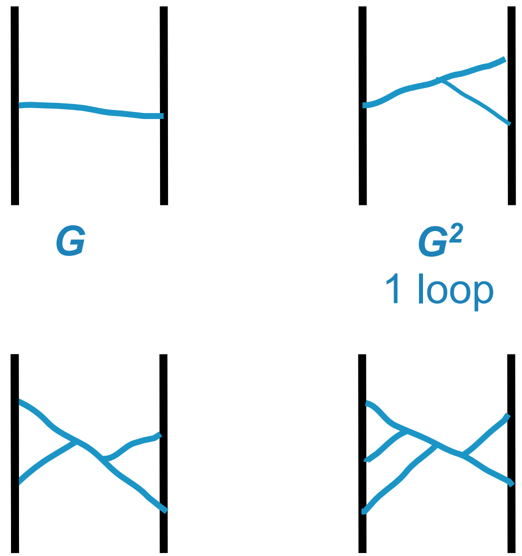

G G^2 1 loop

G^3 2 loops G^4 3 loops

Effective dynamics

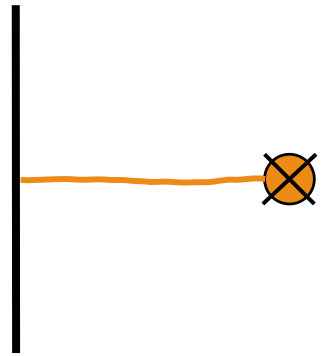

$g_{\mu\nu}^{\text{eff}}$

$$S = -\int \mu ds + \dots$$

$$H = H_0 + \left(G H_1 + \frac{G^2}{c^2} H_2 + \frac{G^3}{c^4} H_3 + \frac{G^4}{c^6} H_4 \right) \left(1 + \frac{1}{c^2} + \dots \right)$$

Effective metric

$$ds_{\text{eff}}^2 = -A(r)dt^2 + B(r)dr^2 + r^2 \left(d\theta^2 + \sin^2\theta d\varphi^2 \right)$$

Two-body/EOB "correspondence": think quantum-mechanically (Wheeler)

Real 2-body system (m_1, m_2) (in the c.o.m. frame)

an effective particle of mass μ in some effective metric $g_{\mu\nu}^{eff}(M)$

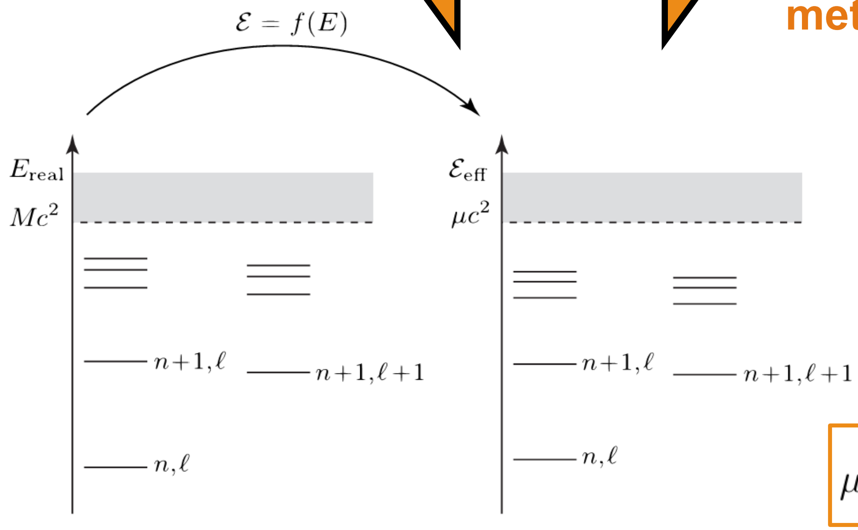

Figure 1: Sketch of the correspondence between the quantized energy levels of the real and effective conservative dynamics. n denotes the 'principal quantum

$$\mu^2 + g_{\rm eff}^{\mu\nu} \frac{\partial S_{\rm eff}}{\partial x^\mu} \frac{\partial S_{\rm eff}}{\partial x^\nu} + \mathcal{O}(p^4) = 0$$

Sommerfeld "Old Quantum Mechanics":

$$J = \ell\hbar = \frac{1}{2\pi} \oint p_\varphi \, d\varphi$$

$$N = n\hbar = I_r + J$$

$$I_r = \frac{1}{2\pi} \oint p_r \, dr$$

$H^{\rm classical}(q,p)$ → $H^{classical}(I_a)$ → $E^{\rm quantum}(I_a = n_a h) = f^{-1}\left[\mathcal{E}_{\rm eff}^{\rm quantum}\left(I_a^{\rm eff} = n_a h\right)\right]$

The EOB energy map

Real 2-body system *(m_1, m_2)*
(in the c.o.m. frame)

an effective particle of
Mass $\mu = m_1 m_2/(m_1+m_2)$ in
some effective
metric $g_{\mu\nu}^{eff}(M)$

Simple energy map

$$\mathcal{E}_{eff} = \frac{s - m_1^2 - m_2^2}{2M}$$

$$s = E_{\mathrm{real}}^2$$

$$H_{\mathrm{EOB}} = M\sqrt{1 + 2\nu\left(\hat{H}_{\mathrm{eff}} - 1\right)}$$

$$\begin{aligned} M &= m_1 + m_2 \\ \nu &= m_1 m_2/(m_1 + m_2)^2 \end{aligned}$$

Explicit form of the EOB effective Hamiltonian

The effective metric $g_{\mu\nu}^{eff}(M)$ at 3PN

$$ds^2 = -A(r)dt^2 + B(r)dr^2 + r^2(d\theta^2 + \sin^2\theta d\varphi^2).$$

where the coefficients are a ν-dependent "deformation" of the Schwarzschild ones:

$$\boxed{A_{3\text{PN}}(R) = 1 - 2u + 2\nu\, u^3 + a_4 \nu\, u^4}$$

$$\boxed{a_4 = \frac{94}{3} - \frac{41}{32}\pi^2 \simeq 18.6879027}$$

$$(A(R)B(R))_{3\text{PN}} = 1 - 6\nu\, u^2 + 2(3\nu - 26)\nu u^3$$

u = GM/(c²r)

Simple effective Hamiltonian

$$\hat{H}_{\text{eff}} \equiv \sqrt{p_{r_*}^2 + A\left(1 + \frac{p_\varphi^2}{r^2} + z_3 \frac{p_{r_*}^4}{r^2}\right)}.$$

$$p_{r_*} = \left(\frac{A}{B}\right)^{1/2} p_r$$

crucial EOB "radial potential" A(r)

2-body Taylor-expanded 3PN Hamiltonian [JS98, DJS00,01]

$$H_{\rm N}(\mathbf{x}_a,\mathbf{p}_a)=\sum_a\frac{\mathbf{p}_a^2}{2\,m_a}-\frac{1}{2}\sum_a\sum_{b\neq a}\frac{G\,m_a\,m_b}{r_{ab}}\,.$$

$$H_{\rm 1PN}(\mathbf{x}_a,\mathbf{p}_a)=-\frac{1}{8}\frac{(\mathbf{p}_1^2)^2}{m_1^3}+\frac{1}{8}\frac{Gm_1m_2}{r_{12}}\left[-12\,\frac{\mathbf{p}_1^2}{m_1^2}+14\,\frac{(\mathbf{p}_1\cdot\mathbf{p}_2)}{m_1m_2}+2\,\frac{(\mathbf{n}_{12}\cdot\mathbf{p}_1)(\mathbf{n}_{12}\cdot\mathbf{p}_2)}{m_1m_2}\right]\quad+\frac{1}{4}\frac{Gm_1m_2}{r_{12}}\frac{G(m_1+m_2)}{r_{12}}+(1\longleftrightarrow 2),$$

1PN

$$\begin{aligned}H_{\rm 2PN}(\mathbf{x}_a,\mathbf{p}_a)=&\frac{1}{16}\frac{(\mathbf{p}_1^2)^3}{m_1^5}+\frac{1}{8}\frac{Gm_1m_2}{r_{12}}\left[5\,\frac{(\mathbf{p}_1^2)^2}{m_1^4}-\frac{11}{2}\frac{\mathbf{p}_1^2\,\mathbf{p}_2^2}{m_1^2m_2^2}-\frac{(\mathbf{p}_1\cdot\mathbf{p}_2)^2}{m_1^2m_2^2}+5\,\frac{\mathbf{p}_1^2\,(\mathbf{n}_{12}\cdot\mathbf{p}_2)^2}{m_1^2m_2^2}\right.\\
&\left.-6\,\frac{(\mathbf{p}_1\cdot\mathbf{p}_2)\,(\mathbf{n}_{12}\cdot\mathbf{p}_1)(\mathbf{n}_{12}\cdot\mathbf{p}_2)}{m_1^2m_2^2}-\frac{3}{2}\frac{(\mathbf{n}_{12}\cdot\mathbf{p}_1)^2(\mathbf{n}_{12}\cdot\mathbf{p}_2)^2}{m_1^2m_2^2}\right]\\
&+\frac{1}{4}\frac{G^2m_1m_2}{r_{12}^2}\left[m_2\left(10\frac{\mathbf{p}_1^2}{m_1^2}+19\frac{\mathbf{p}_2^2}{m_2^2}\right)-\frac{1}{2}(m_1+m_2)\frac{27\,(\mathbf{p}_1\cdot\mathbf{p}_2)+6\,(\mathbf{n}_{12}\cdot\mathbf{p}_1)(\mathbf{n}_{12}\cdot\mathbf{p}_2)}{m_1m_2}\right]\\
&-\frac{1}{8}\frac{Gm_1m_2}{r_{12}}\frac{G^2(m_1^2+5m_1m_2+m_2^2)}{r_{12}^2}+(1\longleftrightarrow 2).\end{aligned}$$

2PN

$$\begin{aligned}H^{\rm reg}_{\rm 3PN}(\mathbf{x}_a,\mathbf{p}_a)=&-\frac{5}{128}\frac{(\mathbf{p}_1^2)^4}{m_1^7}+\frac{1}{32}\frac{Gm_1m_2}{r_{12}}\left[-14\,\frac{(\mathbf{p}_1^2)^3}{m_1^6}+4\,\frac{\big((\mathbf{p}_1\cdot\mathbf{p}_2)^2+4\,\mathbf{p}_1^2\,\mathbf{p}_2^2\big)\mathbf{p}_1^2}{m_1^4m_2^2}+\frac{\big(\mathbf{p}_1^2\,\mathbf{p}_2^2-2\,(\mathbf{p}_1\cdot\mathbf{p}_2)^2\big)(\mathbf{p}_1\cdot\mathbf{p}_2)}{m_1^3m_2^3}\right.\\
&-10\,\frac{\big(\mathbf{p}_1^2\,(\mathbf{n}_{12}\cdot\mathbf{p}_2)^2+\mathbf{p}_2^2\,(\mathbf{n}_{12}\cdot\mathbf{p}_1)^2\big)\mathbf{p}_1^2}{m_1^4m_2^2}+24\,\frac{\mathbf{p}_1^2\,(\mathbf{p}_1\cdot\mathbf{p}_2)(\mathbf{n}_{12}\cdot\mathbf{p}_1)(\mathbf{n}_{12}\cdot\mathbf{p}_2)}{m_1^4m_2^2}+2\,\frac{\mathbf{p}_1^2\,(\mathbf{p}_1\cdot\mathbf{p}_2)(\mathbf{n}_{12}\cdot\mathbf{p}_2)^2}{m_1^3m_2^3}\\
&+\frac{\big(7\,\mathbf{p}_1^2\,\mathbf{p}_2^2-10\,(\mathbf{p}_1\cdot\mathbf{p}_2)^2\big)(\mathbf{n}_{12}\cdot\mathbf{p}_1)(\mathbf{n}_{12}\cdot\mathbf{p}_2)}{m_1^3m_2^3}+6\,\frac{\mathbf{p}_1^2\,(\mathbf{n}_{12}\cdot\mathbf{p}_1)^2(\mathbf{n}_{12}\cdot\mathbf{p}_2)^2}{m_1^4m_2^2}\\
&\left.+15\,\frac{(\mathbf{p}_1\cdot\mathbf{p}_2)(\mathbf{n}_{12}\cdot\mathbf{p}_1)^2(\mathbf{n}_{12}\cdot\mathbf{p}_2)^2}{m_1^3m_2^3}-18\,\frac{\mathbf{p}_1^2\,(\mathbf{n}_{12}\cdot\mathbf{p}_1)(\mathbf{n}_{12}\cdot\mathbf{p}_2)^3}{m_1^3m_2^3}+5\,\frac{(\mathbf{n}_{12}\cdot\mathbf{p}_1)^3(\mathbf{n}_{12}\cdot\mathbf{p}_2)^3}{m_1^3m_2^3}\right]\\
&+\frac{G^2m_1m_2}{r_{12}^2}\left[\frac{1}{16}(m_1-27m_2)\frac{(\mathbf{p}_1^2)^2}{m_1^4}-\frac{115}{16}m_1\frac{\mathbf{p}_1^2\,(\mathbf{p}_1\cdot\mathbf{p}_2)}{m_1^3m_2}+\frac{1}{48}m_2\frac{25\,(\mathbf{p}_1\cdot\mathbf{p}_2)^2+371\,\mathbf{p}_1^2\,\mathbf{p}_2^2}{m_1^2m_2^2}\right.\\
&+\frac{17}{16}\frac{\mathbf{p}_1^2(\mathbf{n}_{12}\cdot\mathbf{p}_1)^2}{m_1^3}-\frac{1}{8}m_1\frac{\big(15\,\mathbf{p}_1^2\,(\mathbf{n}_{12}\cdot\mathbf{p}_2)+11\,(\mathbf{p}_1\cdot\mathbf{p}_2)\,(\mathbf{n}_{12}\cdot\mathbf{p}_1)\big)(\mathbf{n}_{12}\cdot\mathbf{p}_1)}{m_1^3m_2}+\frac{5}{12}\frac{(\mathbf{n}_{12}\cdot\mathbf{p}_1)^4}{m_1^3}\\
&-\frac{3}{2}m_1\frac{(\mathbf{n}_{12}\cdot\mathbf{p}_1)^3(\mathbf{n}_{12}\cdot\mathbf{p}_2)}{m_1^3m_2}+\frac{125}{12}m_2\frac{(\mathbf{p}_1\cdot\mathbf{p}_2)\,(\mathbf{n}_{12}\cdot\mathbf{p}_1)(\mathbf{n}_{12}\cdot\mathbf{p}_2)}{m_1^2m_2^2}+\frac{10}{3}m_2\frac{(\mathbf{n}_{12}\cdot\mathbf{p}_1)^2(\mathbf{n}_{12}\cdot\mathbf{p}_2)^2}{m_1^2m_2^2}\\
&\left.-\frac{1}{48}(220m_1+193m_2)\frac{\mathbf{p}_1^2(\mathbf{n}_{12}\cdot\mathbf{p}_2)^2}{m_1^2m_2^2}\right]+\frac{G^3m_1m_2}{r_{12}^3}\left[-\frac{1}{48}\left(466\,m_1^2+\left(473-\frac{3}{4}\pi^2\right)m_1m_2+150\,m_2^2\right)\frac{\mathbf{p}_1^2}{m_1^2}\right.\\
&+\frac{1}{16}\left(77(m_1^2+m_2^2)+\left(143-\frac{1}{4}\pi^2\right)m_1m_2\right)\frac{(\mathbf{p}_1\cdot\mathbf{p}_2)}{m_1m_2}+\frac{1}{16}\left(61\,m_1^2-\left(43+\frac{3}{4}\pi^2\right)m_1m_2\right)\frac{(\mathbf{n}_{12}\cdot\mathbf{p}_1)^2}{m_1^2}\\
&\left.+\frac{1}{16}\left(21(m_1^2+m_2^2)+\left(119+\frac{3}{4}\pi^2\right)m_1m_2\right)\frac{(\mathbf{n}_{12}\cdot\mathbf{p}_1)(\mathbf{n}_{12}\cdot\mathbf{p}_2)}{m_1m_2}\right]\\
&+\frac{1}{8}\frac{G^4m_1m_2^3}{r_{12}^4}\left[\left(\frac{227}{3}-\frac{21}{4}\pi^2\right)m_1+m_2\right]+(1\longleftrightarrow 2).\end{aligned}\tag{12}$$

3PN

Hamilton's equation + radiation reaction

$$\frac{dr}{dt} = \left(\frac{A}{B}\right)^{1/2} \frac{\partial \hat{H}_{\rm EOB}}{\partial p_{r_*}} \,,$$

$$\frac{dp_{r_*}}{dt} = -\left(\frac{A}{B}\right)^{1/2} \frac{\partial \hat{H}_{\rm EOB}}{\partial r} \,,$$

$$\Omega \equiv \frac{d\varphi}{dt} = \frac{\partial \hat{H}_{\rm EOB}}{\partial p_\varphi} \,,$$

$$\frac{dp_\varphi}{dt} = \hat{\mathcal{F}}_\varphi \,.$$

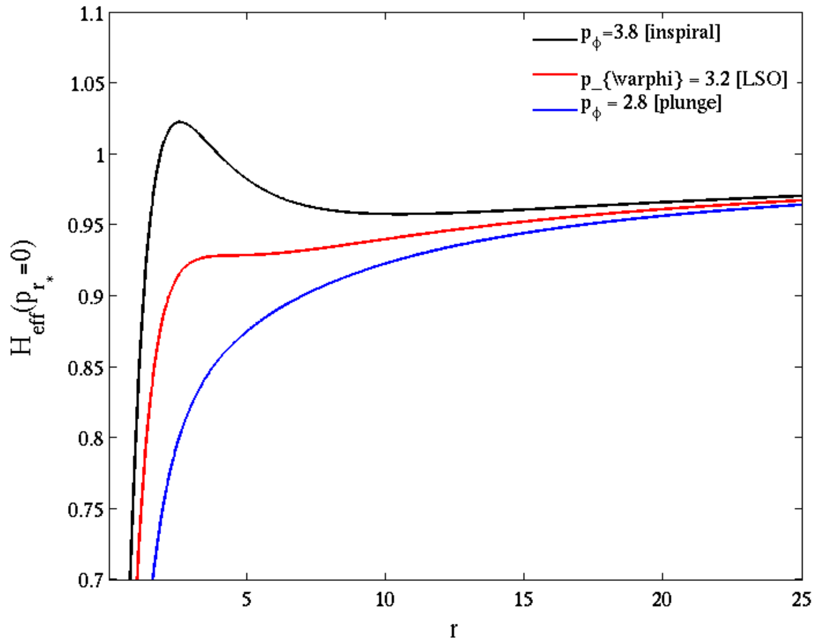

The system must lose mechanical angular momentum

Use PN-expanded result for ***GW angular momentum flux*** as a starting point.
Needs resummation to have a better behavior during late-inspiral and plunge.

PN calculations are done in the circular approximation

$$\hat{\mathcal{F}}_\varphi^{\rm Taylor} = -\frac{32}{5}\,\nu\,\Omega^5\,r_\omega^4\,\hat{F}^{\rm Taylor}(v_\varphi)$$

Parameter-dependent

EOB 1.* **[DIS 1998, DN07]**

Parameter -free:

EOB 2.0 **[DIN 2008, DN09]**

EOB 2.0: new resummation procedures (DN07, DIN 2008)

- Resummation of the waveform **multipole by multipole**
- **Factorized** waveform for any (l,m) at the highest available PN order (start from PN results of Blanchet et al.)

Next-to-Quasi-Circular correction

$$h_{\ell m} = h^{(N)}_{\ell m} \hat{h}^{(\epsilon)}_{\ell m} f^{\rm NQC}_{\ell m}$$

Newtonian x PN-correction

remnant phase correction

$$\hat{h}^{(\epsilon)}_{\ell m} = \hat{S}^{(\epsilon)}_{\rm eff} T_{\ell m} e^{{\rm i}\delta_{\ell m}} \rho^{\ell}_{\ell m}$$

remnant modulus correction:

- l-th power of the (expanded) l-th root of f_{lm}
- improves the behavior of PN corrections

The “Tail factor”

$$\boxed{T_{\ell m} = \frac{\Gamma(\ell + 1 - 2{\rm i}\hat{\hat{k}})}{\Gamma(\ell+1)} e^{\pi \hat{\hat{k}}} e^{2{\rm i}\hat{\hat{k}} \log(2kr_0)}}$$

Effective source:

EOB (effective) energy (even-parity)

Angular momentum (odd-parity)

resums an infinite number of leading logarithms in tail effects

Radiation reaction: parameter-free resummation

$$\mathcal{F}_\varphi \equiv -\frac{1}{8\pi\,\Omega}\sum_{\ell=2}^{\ell_{\max}}\sum_{m=1}^{\ell}(m\,\Omega)^2\,|R\,h_{\ell m}^{(\epsilon)}|^2$$

$$h_{\ell m} = h_{\ell m}^{(N)}\hat{h}_{\ell m}^{(\epsilon)} f_{\ell m}^{\rm NQC}$$

$$\hat{h}_{\ell m}^{(\epsilon)} = \hat{S}_{\rm eff}^{(\epsilon)} T_{\ell m} e^{{\rm i}\delta_{\ell m}}\rho_{\ell m}^{\ell}$$

$$\begin{aligned}\rho_{22}(x;\nu) = 1 &+ \left(\frac{55\nu}{84}-\frac{43}{42}\right)x + \left(\frac{19583\nu^2}{42336}-\frac{33025\nu}{21168}-\frac{20555}{10584}\right)x^2\\ &+\left(\frac{10620745\nu^3}{39118464}-\frac{6292061\nu^2}{3259872}+\frac{41\pi^2\nu}{192}-\frac{48993925\nu}{9779616}-\frac{428}{105}\mathrm{eulerlog}_2(x)+\frac{1556919113}{122245200}\right)x^3\\ &+\left(\frac{9202}{2205}\mathrm{eulerlog}_2(x)-\frac{387216563023}{160190110080}\right)x^4+\left(\frac{439877}{55566}\mathrm{eulerlog}_2(x)-\frac{16094530514677}{533967033600}\right)x^5+\mathcal{O}(x^6),\end{aligned}$$

- Different possible representations of the residual amplitude correction [Padé]

Test-mass

(Comparing fluxes, circular orbits)

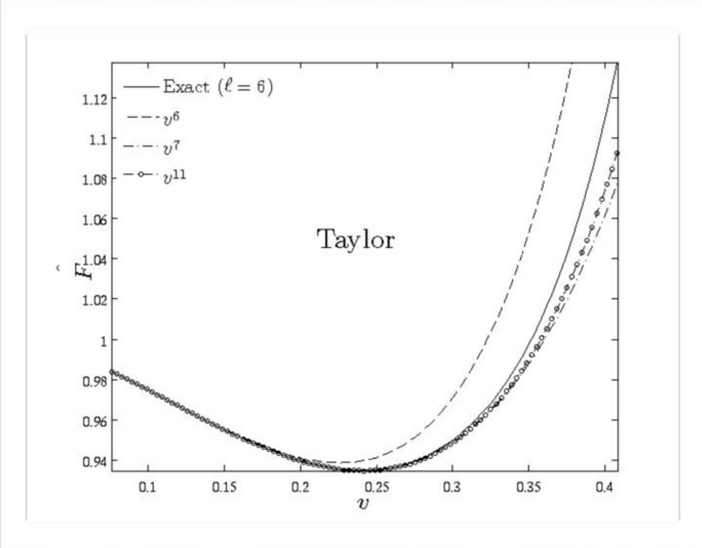

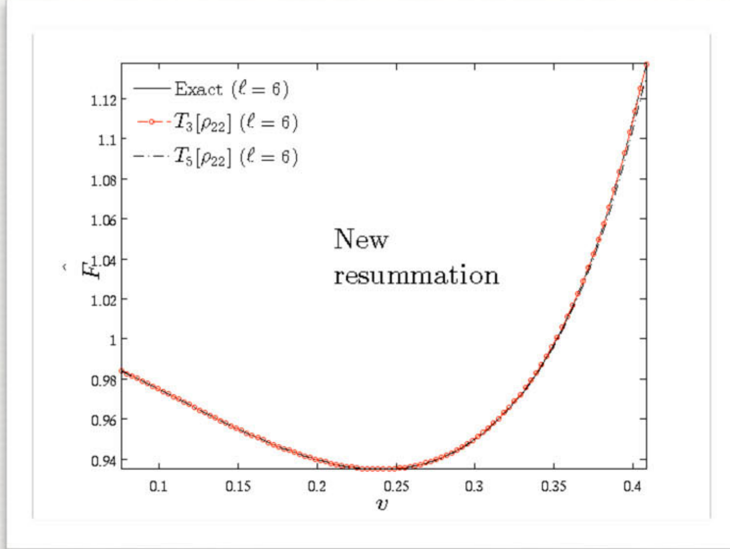

Equal-mass

(Comparing non-resummed & EOB-resummed *amplitudes* to Caltech-Cornell BBH data)

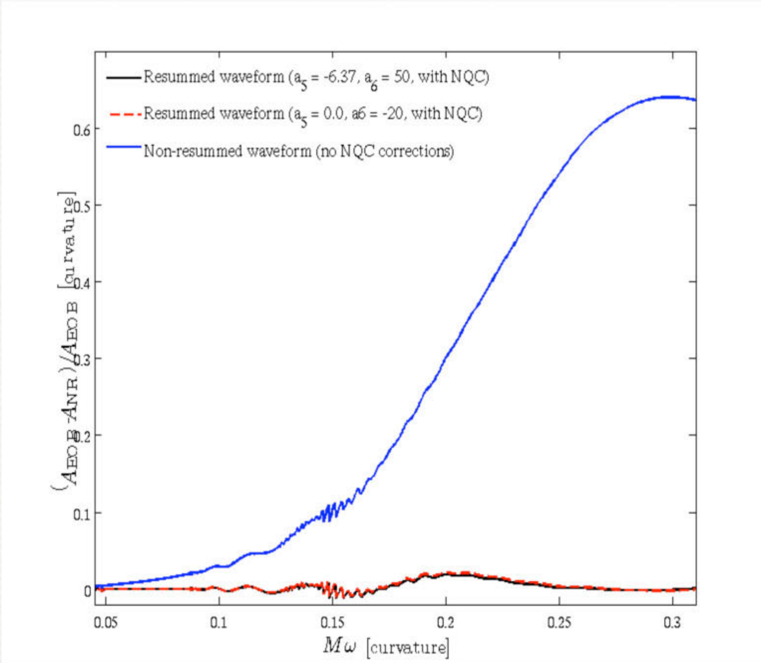

Extending EOB beyond current analytical knowledge

Introducing (a5, a6) parametrizing 4-loop and 5-loop effects

$$\boxed{A(u; a_5, a_6, \nu) \equiv P_5^1[A^{3\mathrm{PN}}(u) + \nu a_5 u^5 + \nu a_6 u^6]}$$

Introducing next-to-quasi-circular corrections to the quadrupolar GW amplitude

$$f_{22}^{\mathrm{NQC}}(a_1, a_2) = 1 + a_1\, p_{r_*}^2/(r\Omega)^2 + a_2\, \ddot{r}/r\,\Omega^2$$

Use Caltech-Cornell [inspiral-plunge] NR data to constrain ***(a_5,a_6)***

A wide region of correlated values ***(a_5,a_6)*** exists where the phase difference can be reduced at the level of the numerical error (<0.02 radians) during the inspiral

EOB-NR: NONSPINNING BINARIES

Need calibration of high-order PN effects with NR data: q=1,2&4 TD&AN, et al. (2009)

$$A(u, a_5, a_6; \nu) = P^1_5[A^{3\mathrm{PN}}(u;\nu) + \nu a_5 u^5 + \nu a_6 u^6]$$

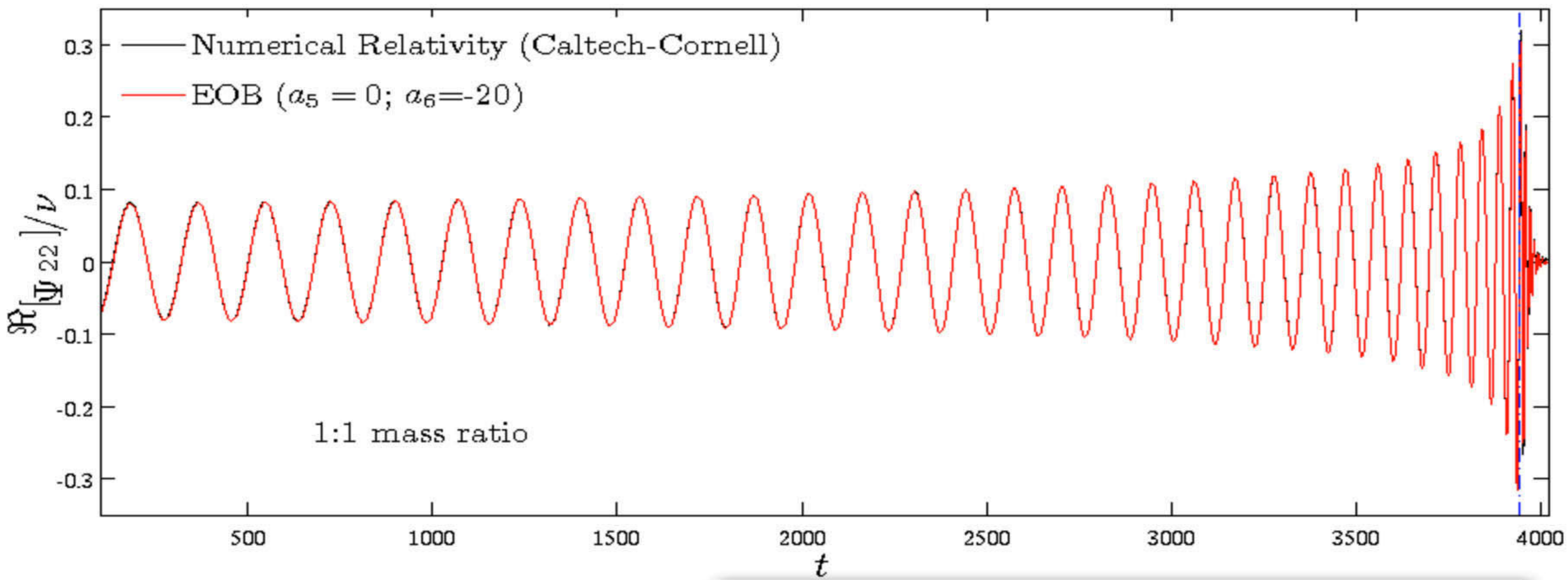

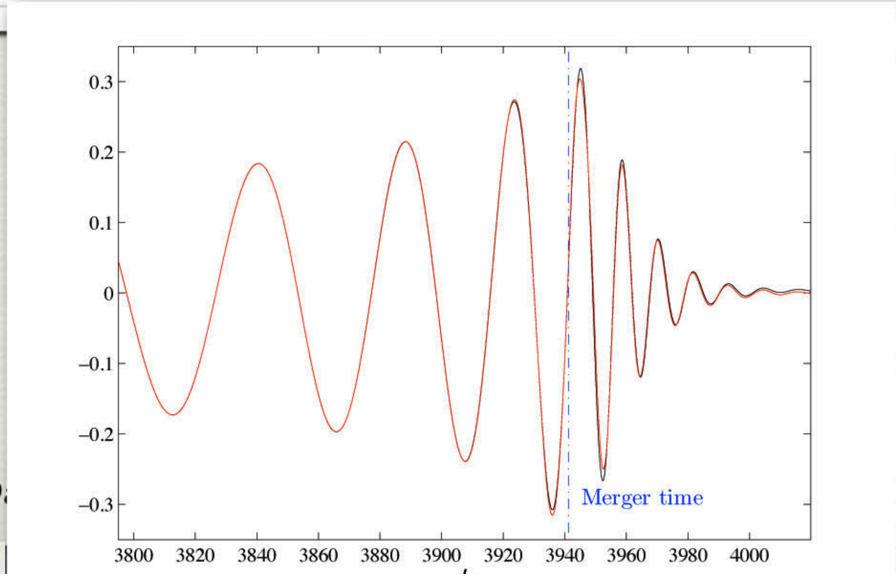

Da

EOB-NR: NONSPINNING BINARIES

$$A(u, a_5, a_6; \nu) = P_5^1[A^{3PN}(u;\nu) + \nu a_5 u^5 + \nu a_6 u^6]$$

q=1,2,3,4 and 6

(Buonanno, Pan et al. 2011)

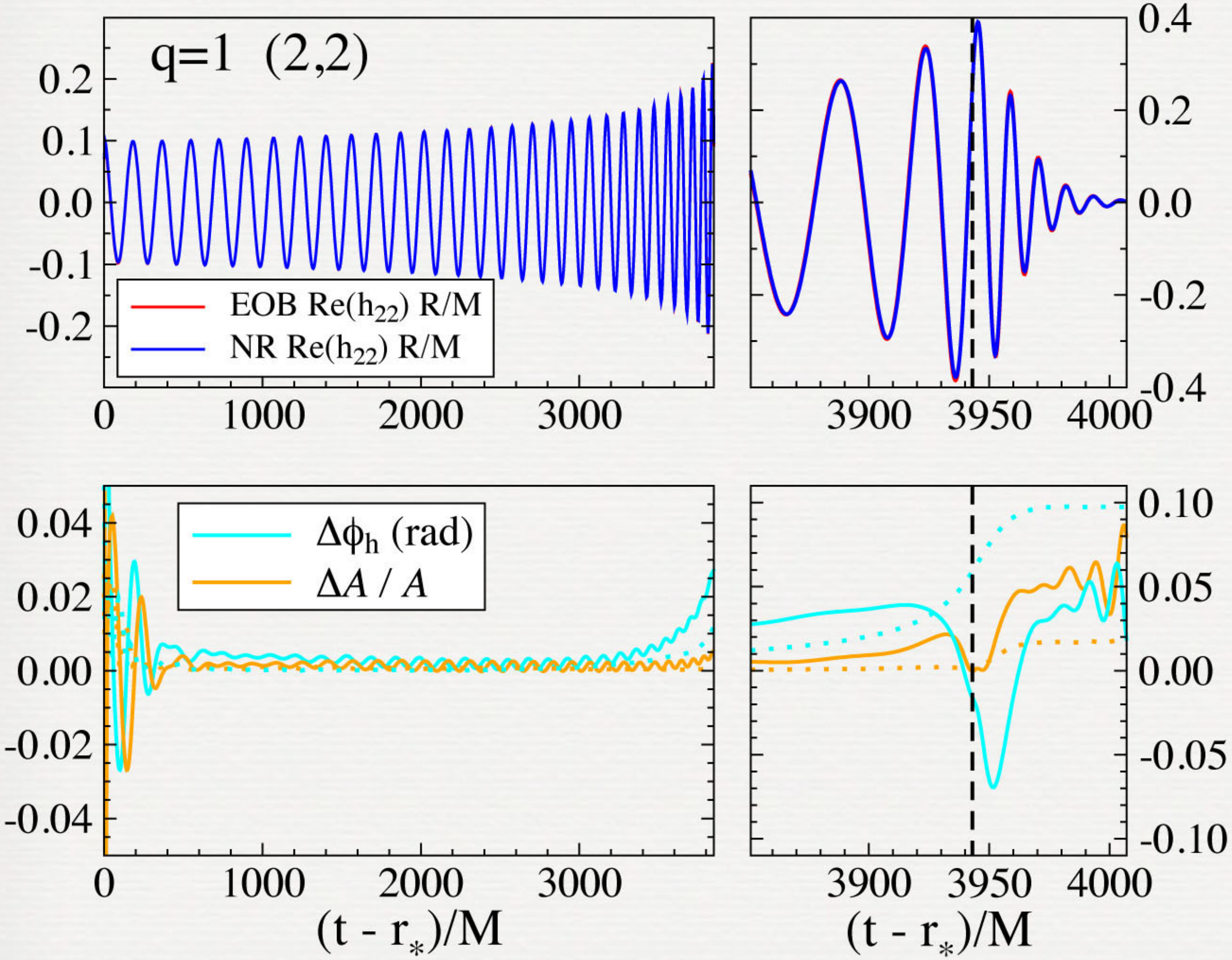

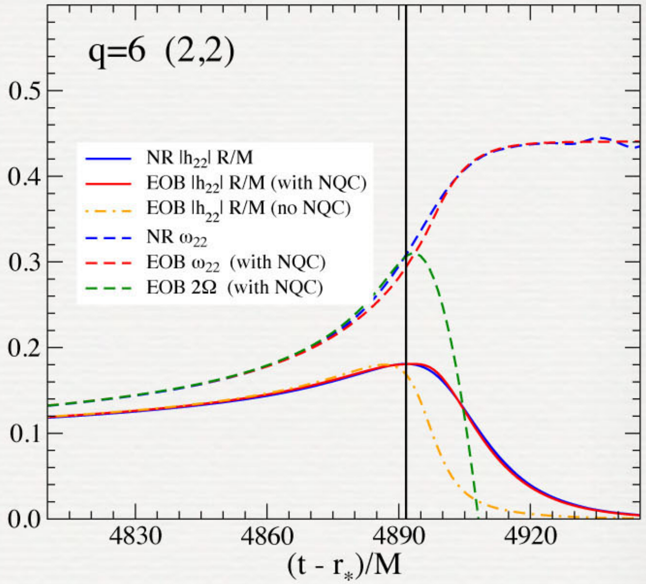

RECENT THEORETICAL DEVELOPMENTS: LOGS

Recently computed 4PN and 5PN terms in the A(u) function:

(Damour 2010, Blanchet et al. 2010, Akcay, Barack, Damour & Sago 2012, Barausse, Buonanno & Le Tiec 2012, Jaranowski & Schaefer 2013, Bini& Damour 2013)

$$A^{\text{Taylor}}(u) = 1 - 2u + 2\nu u^3 + \left(\frac{94}{3} - \frac{41}{32}\pi^2\right)\nu u^4 + \nu[a_5^c(\nu) + a_5^{\ln}(\nu)\ln u]u^5 + \nu[a_6^c(\nu) + a_6^{\ln}(\nu)\ln u]u^6$$

$$a_5^{\ln}(\nu) = \frac{64}{5}$$

$$a_6^{\ln}(\nu) = -\frac{7004}{105} - \frac{144}{5}\nu$$

$$a_5^c(\nu) = -\frac{4237}{60} + \frac{2275}{512}\pi^2 + \frac{256}{5}\ln 2 + \frac{128}{5}\gamma + \left(-\frac{221}{6} + \frac{41}{32}\pi^2\right)\nu$$

The 5PN nonlogarithmic terms are analytically unknown.
Used as "effective" parameters to be determined / constrained using NR waveform data

The current EOB potential (with logs):

$$A(u;\nu;a_5^c,a_6^c) = P_5^1[A^{\text{Taylor}}(u)]$$

Main EOB radial potential A(u, v)

Equal- mass case : v = ¼ ; u = GM/c^2R

v-deformation of Schwarzschild $A_S(u) = 1 – 2M/R = 1 – 2u$

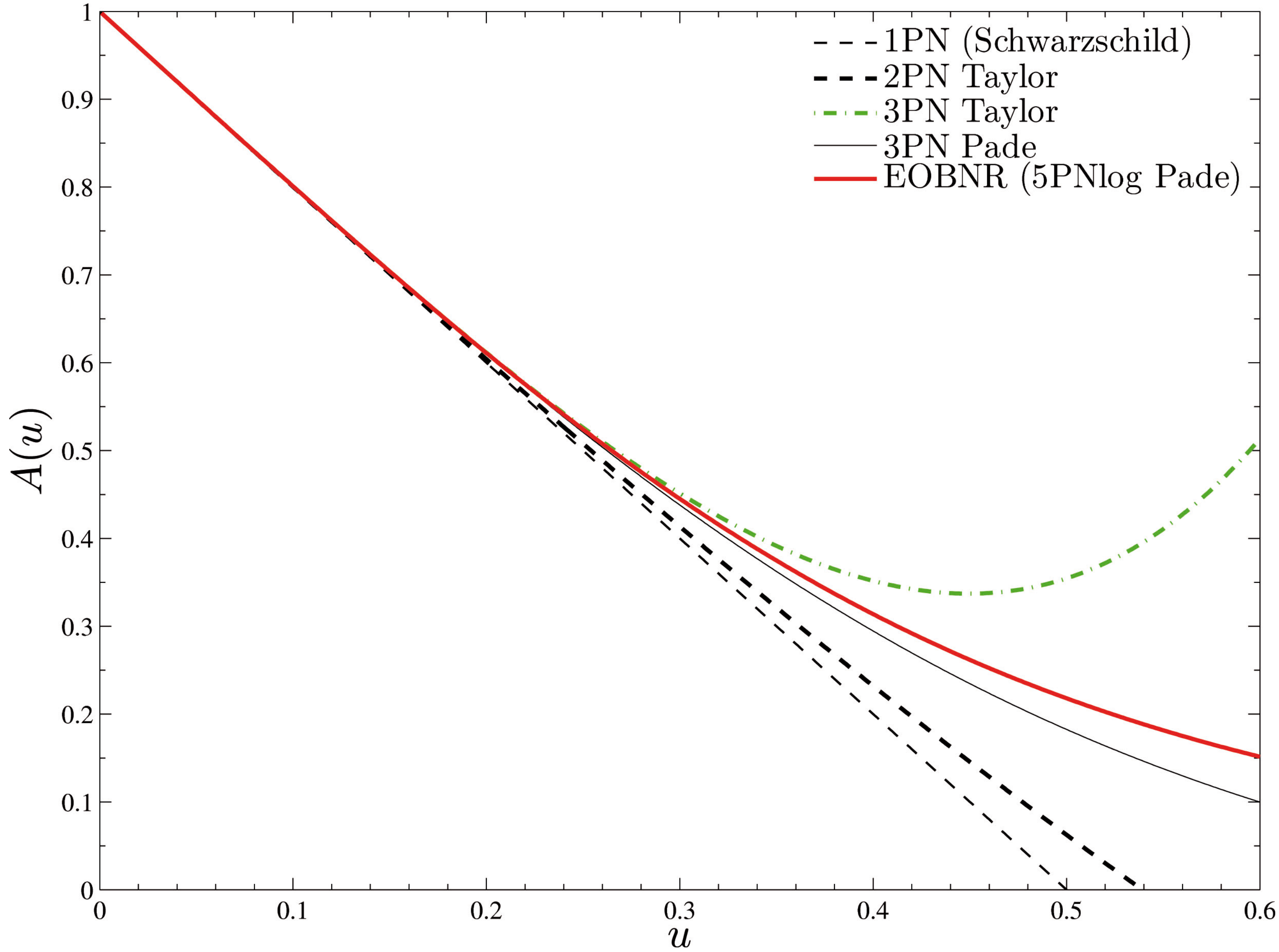

ENERGY AND ANGULAR MOMENTUM IN NONSPINNING BLACK-HOLE BINARIES: E(J)

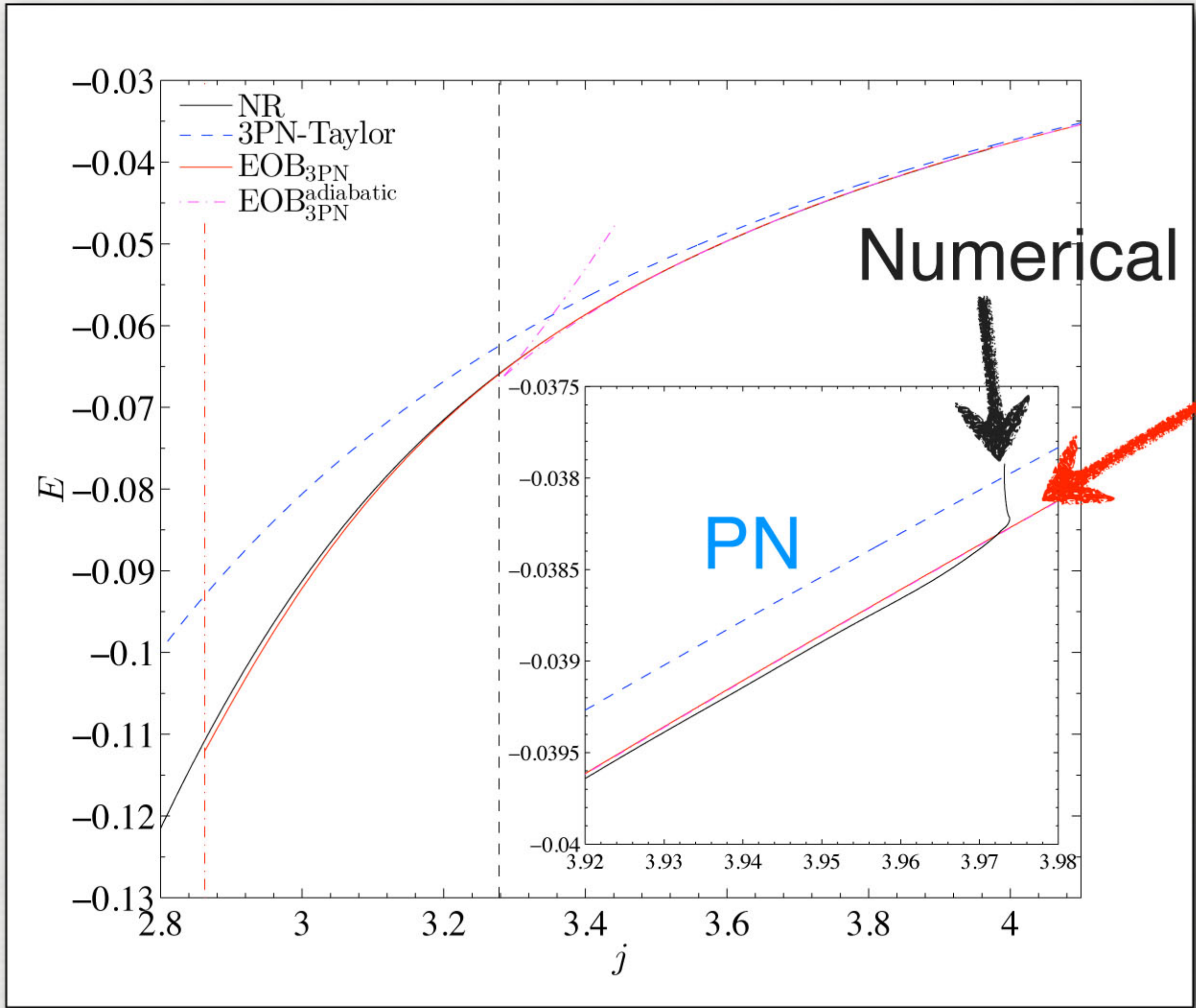

Damour,Nagar,Pollney,Reisswig 2012

EOB-analytical

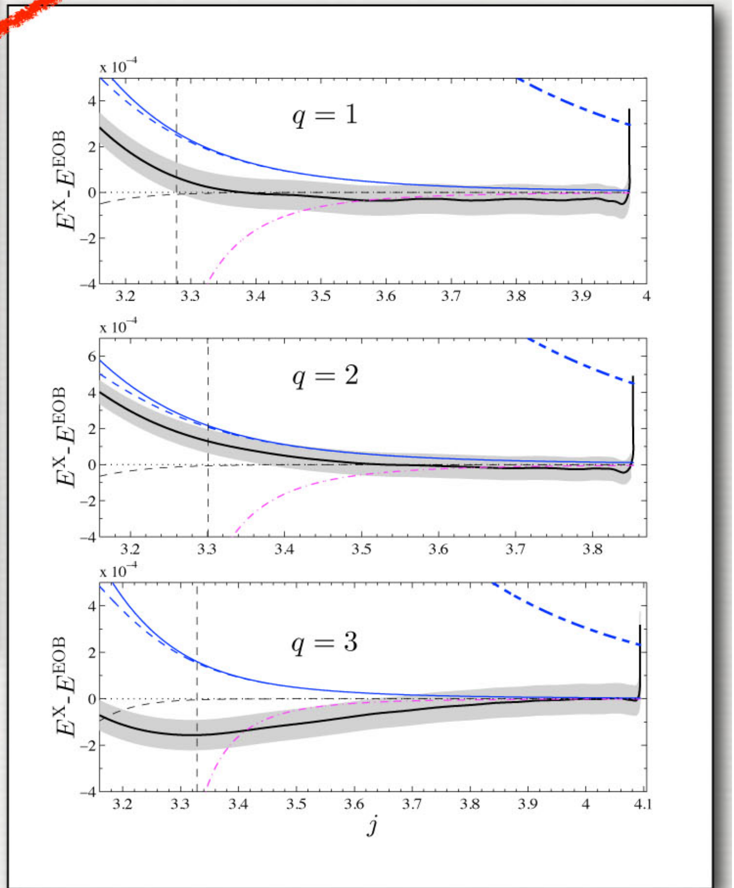

$$j = |\vec{j}_0^{\mathrm{ADM}} - \Delta \vec{j}_{\mathrm{GWs}}|$$

$$E = E_0^{\mathrm{ADM}} - \Delta E_{\mathrm{GWs}}$$

ϱ(x) and periastron advance in (comparable-mass) Black Hole binaries (Le Tiec et al. 2011)

K(x)= Ω_ϕ/Ω_r;   x=(M Ω_ϕ)^(2/3)

$$K_{\rm EOB} = \sqrt{\frac{A'_p(u)}{D(u)\Delta(u)}},$$

where $A'_p = \mathrm{d}A_p/\mathrm{d}u$, and $\Delta = A_pA'_p + 2u(A'_p)^2 - uA_pA''_p$

$$K^{\nu}_{\rm GSF} = \frac{1}{\sqrt{1-6x}}\left[1 - \frac{\nu}{2}\frac{\rho(x)}{1-6x} + \mathcal{O}(\nu^2)\right],$$

3

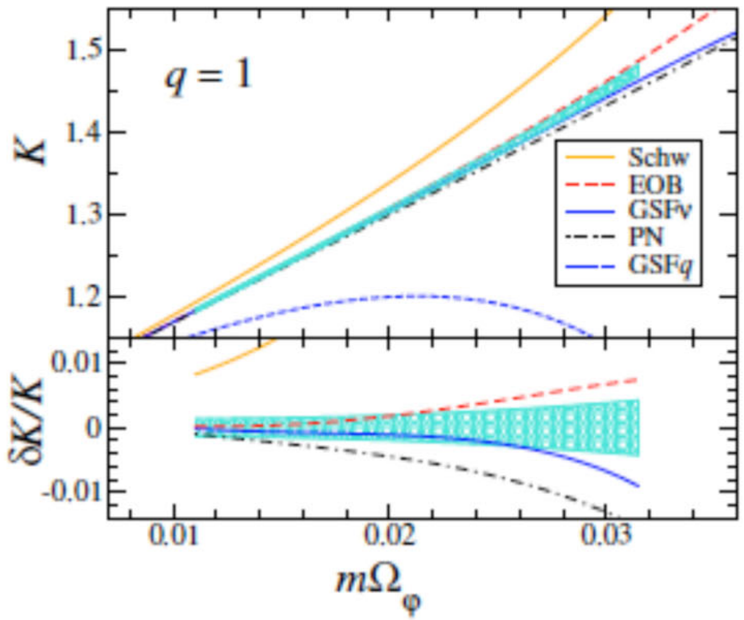

FIG. 1: The periastron advance K of an equal mass black hole binary, in the limit of zero eccentricity, as a function of the orbital frequency Ω_φ of the circular motion. The NR results are indicated by the cyan-shaded region. The PN and EOB results are valid at 3PN order. The lower panel shows the relative difference $\delta K/K \equiv (K - K_{\rm NR})/K_{\rm NR}$.

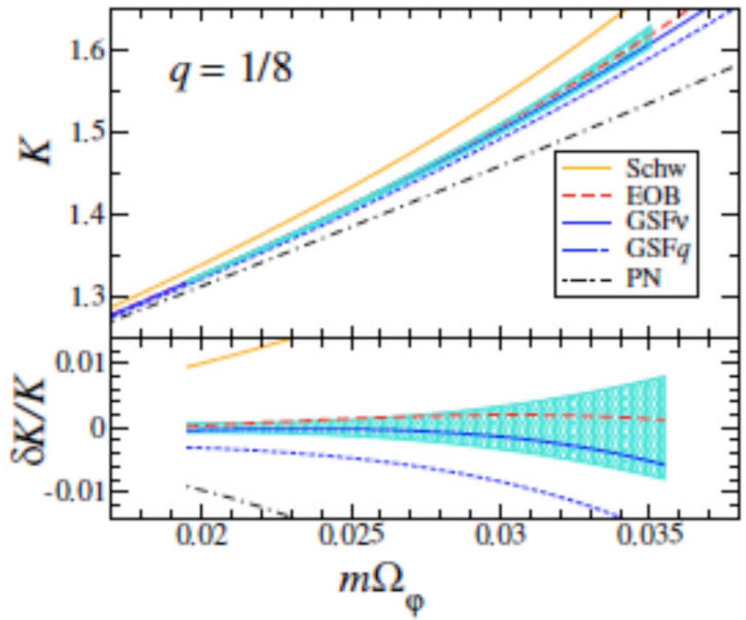

FIG. 2: Same as in Fig. 1, but for a mass ratio $q = 1/8$. Note that for an orbital frequency $m\Omega_\varphi \sim 0.03$, corresponding to a separation $r \sim 10m$, the periastron advance reaches half an orbit per radial period.

Since $\rho(x) > 0$ for all stable circular orbits, the $\mathcal{O}(q)$ GSF

EOB-NR : SPINNING BINARIES

Theory : Damour 01 Damour Jaranowski Schaefer 07; Barausse Buonanno 10; Nagar 11…

Waveform resummation with spin : Pan et al. (2010)

AR/NR comparison : Pan et al. 09, Taracchini et al. 12, Pan et al. 13

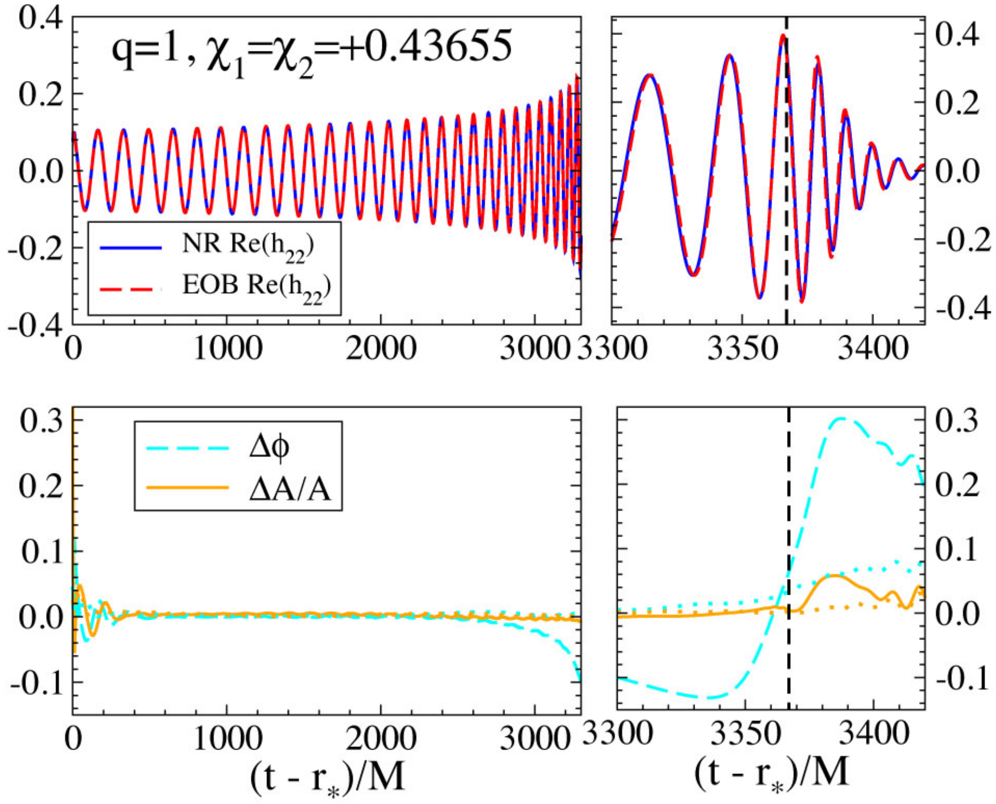

FIG. 6: Same as in Fig. 3 but for $q = 1$, $\chi_1 = \chi_2 = +0.43756$.

EOB-NR : PRECESSING SPINNING BINARIES

Pan et al. 13

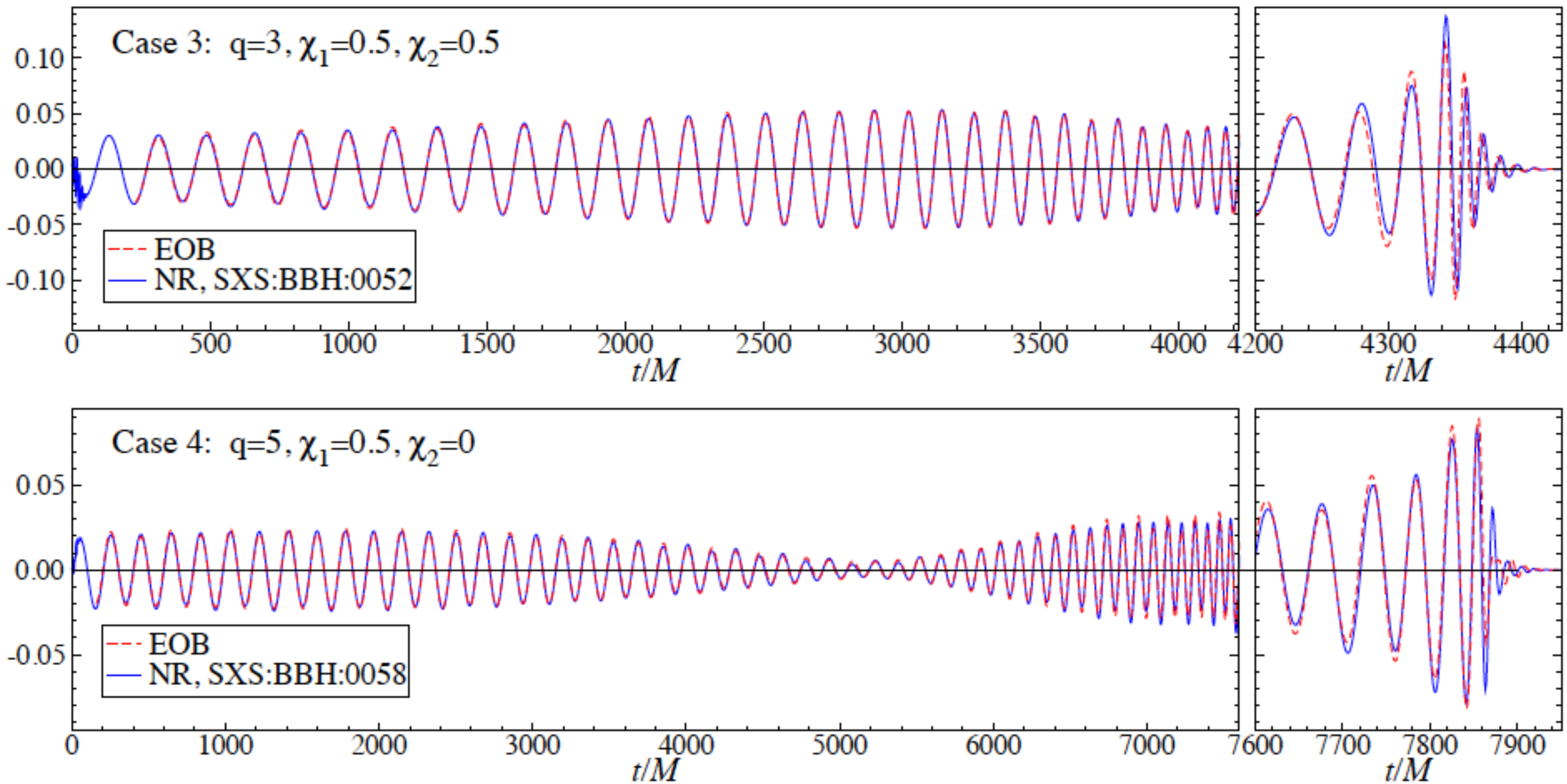

A catalog of 171 high-quality binary black-hole simulations for gravitational-wave astronomy [arXiv: 1304.6077]

Abdul H. Mroué,[1] Mark A. Scheel,[2] Béla Szilágyi,[2] Harald P. Pfeiffer,[1] Michael Boyle,[3] Daniel A. Hemberger,[3] Lawrence E. Kidder,[3] Geoffrey Lovelace,[4,2] Sergei Ossokine,[1,5] Nicholas W. Taylor,[2] Anıl Zenginoğlu,[2] Luisa T. Buchman,[2] Tony Chu,[1] Evan Foley,[4] Matthew Giesler,[4] Robert Owen,[6] and Saul A. Teukolsky[3]

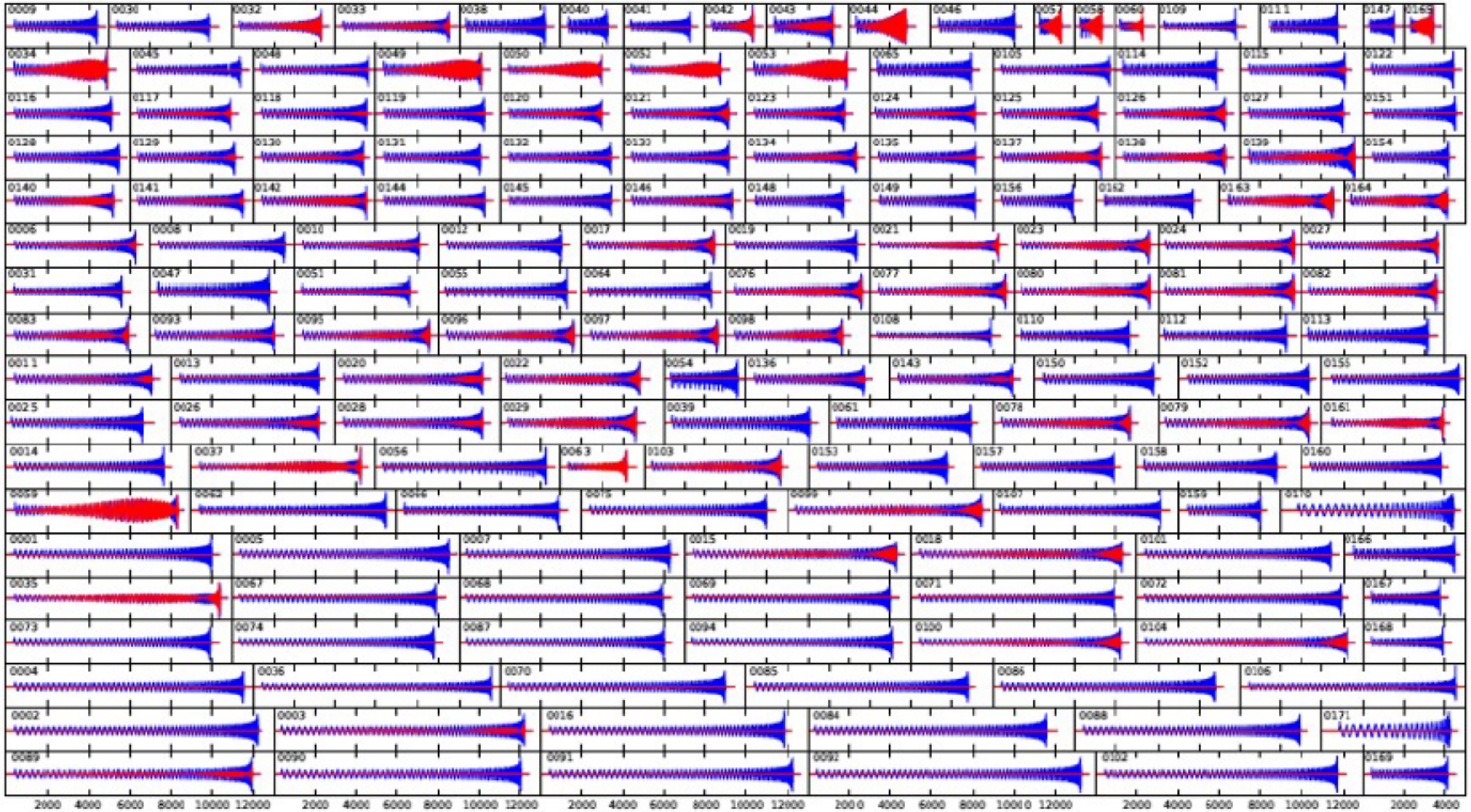

FIG. 3: Waveforms from all simulations in the catalog. Shown here are h_+ (blue) and $h_\times$ (red) in a sky direction parallel to the initial orbital plane of each simulation. All plots have the same horizontal scale, with each tick representing a time interval of $2000M$, where M is the total mass.

Late-inspiral and coalescence of binary neutron stars (BNS)

Inspiralling (and merging) Binary Neutron Star (BNS) systems: important and “secure” targets for GW detectors

Recent progress in BNS and BHNS numerical relativity simulations of merger by several groups [Shibata et al., Baiotti et al., Etienne et al., Duez et al., Bernuzzi et al. 12, Hotokezaka et al. 13] See review of J. Faber, Class. Q. Grav. 26 (2009) 114004
Most sensitive band of GW detectors

Need analytical (NR-completed) modelling of the late-inspiral part of the signal before merger [Flanagan&Hinderer 08, Hinderer et al 09, Damour&Nagar 09,10, Binnington&Poisson 09]
Extract EOS information using late-inspiral (& plunge) waveforms, which are sensitive to tidal interaction. Signal within the

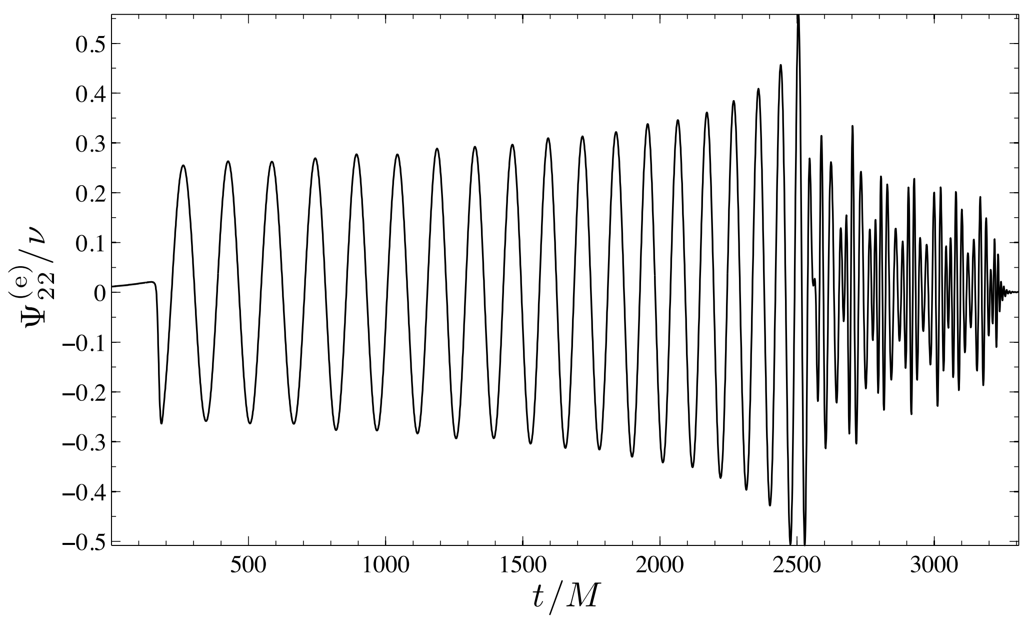

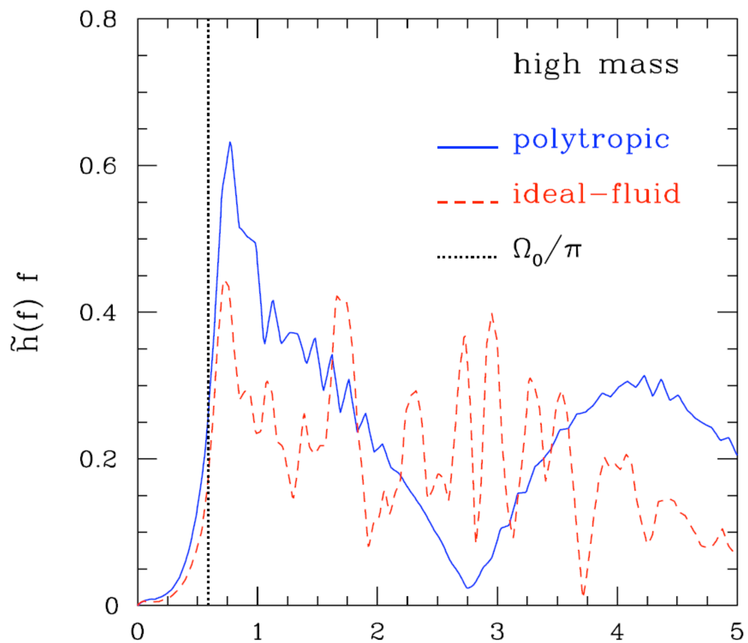

From Baiotti, Giacomazzo & Rezzolla, Phys. Rev. D 78, 084033 (2008)

Binary neutron stars: Tidal effects in EOB

- tidal extension of EOB formalism : non minimal worldline couplings

$$\Delta S_{\text{nonminimal}} = \sum_A \frac{1}{4} \mu_2^A \int ds_A (u^\mu u^\nu R_{\mu\alpha\nu\beta})^2 + \dots$$

Damour, Esposito-Farèse 96, Goldberger, Rothstein 06, Damour, Nagar 09

modification of EOB effective metric + … :

$$\begin{aligned} A(r) &= A^0(r) + A^{\text{tidal}}(r) \\ A^{\text{tidal}}(r) &= -\kappa_2 u^6 (1 + \bar{\alpha}_1 u + \bar{\alpha}_2 u^2 + \dots) + \dots \end{aligned}$$

plus tidal modifications of GW waveform & radiation reaction

➢ Need analytical theory for computing μ_2 , κ_2 as well as $\bar{\alpha}_1, \dots$
[Flanagan&Hinderer 08, Hinderer et al 09, Damour&Nagar 09,10, Binnington&Poisson 09, Damour&Esposito-Farèse10]

➢ Tidal polarizability parameters are measurable in late signals of Advanced-Ligo
[Damour, Nagar and Villain 12, Del Pozzo et al. 13]

Conclusions

- Experimentally, gravitational wave astronomy is about to start. The ground-based network of detectors (LIGO/Virgo/GEO/…) is being updated (ten-fold gain in sensitivity in 2015), and extended (KAGRA, LIGO-India).
- Numerical relativity : Recent breakthroughs (based on a “cocktail” of ingredients : new formulations, constraint damping, punctures, …) allow one to have an accurate knowledge of nonperturbative aspects of the two-body problem (both BBH, BNS and BHNS)
- The Effective One-Body (EOB) method offers a way to upgrade the results of traditional analytical approximation methods (PN and BH perturbation theory) by using new resummation techniques and new ways of combining approximation methods. EOB allows one to analytically describe the FULL coalescence of BBH.
- There exists a complementarity between Numerical Relativity and Analytical Relativity, especially when using the particular resummation of perturbative results defined by the Effective One Body formalism. The NR- tuned EOB formalism is likely to be essential for computing the many thousands of accurate GW templates needed for LIGO/Virgo/...